Original research article

A probabilistic model of relapse in drug addiction

Sayun Mao [a], Tom Chou [a], Maria R. D'Orsogna [a,b,*]

[a] *Department of Computational Medicine, UCLA, Los Angeles, 90095-1766, CA, USA*
[b] *Department of Mathematics, California State University at Northridge, Los Angeles, 91330, CA, USA*

ARTICLE INFO

ABSTRACT

More than 60% of individuals recovering from substance use disorder relapse within one year. Some will resume drug consumption even after decades of abstinence. The cognitive and psychological mechanisms that lead to relapse are not completely understood, but stressful life experiences and external stimuli that are associated with past drug-taking are known to play a primary role. Stressors and cues elicit memories of drug-induced euphoria and the expectation of relief from current anxiety, igniting an intense craving to use again; positive experiences and supportive environments may mitigate relapse. We present a mathematical model of relapse in drug addiction that draws on known psychiatric concepts such as the "positive activation; negative activation" paradigm and the "peak-end" rule to construct a relapse rate that depends on external factors (intensity and timing of life events) and individual traits (mental responses to these events). We analyze which combinations and ordering of stressors, cues, and positive events lead to the largest relapse probability and propose interventions to minimize the likelihood of relapse. We find that the best protective factor is exposure to a mild, yet continuous, source of contentment, rather than large, episodic jolts of happiness.

1. Introduction

Illicit drug abuse remains a major problem in the United States. Despite decades of research and the implementation of policies ranging from harm reduction to punitive measures, drug overdose deaths have increased dramatically over the past 40 years, surpassing 107,000 fatalities in 2022 [1]. According to the 2021 National Survey on Drug Use and Health (NSDUH) about 3.3% of the population aged 12 and above misused opioids in 2021, the latest year for which data is available [2].

Our understanding of substance abuse has also evolved in the past 40 years: addiction, once viewed as a lifestyle choice, is now considered a chronic brain disease characterized by the compulsive seeking and using of drugs despite harmful consequences. Drugs change the neurocircuitry of the brain reward system leading to distortions in how non-drug rewards are processed, diminished self-control, increased sensitivity to stressful events, and the prioritization of drug consumption above all. Over time, tolerance emerges so that for pleasurable sensations to persist or for withdrawal symptoms to dampen, one must increase dosage or intake frequency. Since drug-induced damage to the brain is long-lasting and structural, treatment is a complex process, spanning several years and necessitating behavioral and pharmacological approaches [3]. While detoxification requires a few weeks, remaining sober over a lifetime is challenging: according to the National Institute of Drug Abuse (NIDA) more than 60% of those with substance use disorder relapse within one year [4–6]. The likelihood of relapse is highest in the first months after detoxification [7]; however, relapse is possible even after many years of abstinence [8]. Since those in recovery may have lost their previously built tolerance, de-novo consumption, even in smaller amounts than during active use, may cause overdoses.

Given the severity of the problem, it is important to understand the psychological, behavioral and environmental factors that characterize drug use [9–11]. Many studies have been developed over the years to illustrate the process of addiction, utilizing psychiatric concepts, brain imaging studies, and behavioral surveys [12–19]. Forecasting tools and data analyses have also been presented [20–22]. There is however no explicit quantitative framework to describe the cognitive processes behind relapsing, although the presence of emotional stressors and sensory cues are known to be major influences [23–28].

Among the most vivid memories of addicts (and former addicts) is the pleasure associated with the first time drugs were consumed, often the most euphoric part of the drug-taking experience. "Chasing the first high" is a common refrain, regardless of how far in the past the first high occurred. This aligns with the so-called "peak-end" rule according to which the memory of a past experience is biased by its most emotionally intense period (the high in this case), and its ending [29]. Other less intense periods, or even the entire duration of the experience, do not carry as much mnemonic weight [30]. Relapses may be triggered by stressful events that lead to the retrieval

of euphoric drug-related memories, such as the first high, and to the anticipation of future euphoria if drugs are consumed again [31]. Drugs are viewed as a way to alleviate the negative affects induced by current stressors and to increase short term wellbeing [32]. External cues such as persons, objects, locations, situations connected to past drug use may also evoke memories associated with prior drug consumption and pleasure [33,34]. When stressors and/or cues are present, the associations between drug use and pleasure (or mitigation of pain) may lead to intense cravings and relapse [35]. The goal of this work is to create a mathematical framework whereby the relapse likelihood is described as a function of quantities that represent life stressors occurring at various times and with varying intensity, cues and memories related to the previous drug addiction experience, and changes to the neurocircuitry of the former user.

In the next section, we introduce our mathematical model in which the relapse rate is framed in terms of the mental state of the user, drug availability and the presence of cues. Known psychological and behavioral processes associated with addiction, such as reward collection, tolerance, adaptation, and decision-making [17–19,36–38] are integrated into a probabilistic model of relapse events. Most critical of these components is a "mental state" that is driven by positive life experiences, stressors and cues. Predictions of our model, subject to different sequences of positive events, stressors, and cues are shown in Section 3. We end with further discussion and conclusions in Section 4.

2. Dynamical systems model for relapse

2.1. Relapse rates and probabilities

We begin by assuming that drug consumption has ceased and that the individual started recovery at time $t = 0$. At any time $t > 0$ of the recovery phase, the probability per unit time of relapse, defined as the instant the individual breaks sobriety by drug intake, is assumed to be driven by the user's mental state $M(t)$, which can be either positive or negative, the influence $C(t)$ of any external cues that remind the user of past drug taking euphoria, and the current availability of drugs, $I(t)$. Positive values of the mental state $M(t)$ indicate well-being and optimism, and negative values represent discontent and malaise. Drug availability can be described by a continuous variable that represents the ease with which drugs are acquired and consumed. For simplicity, we binarize $I(t)$ so that $I(t) = 1$ indicates that drugs are readily available and $I(t) = 0$ that they cannot be procured. Finally, cues are assumed to amplify the relapse rate via a non-negative motivation term $C(t) \geq 0$. Together, we let $M(t)$, $C(t)$ and $I(t)$ shape the rate of relapse $R(t)$ via

$$R(t) = I(t)R_0 e^{C(t)} e^{-M(t)}. \tag{1}$$

In this model, $R(t)\mathrm{d}t$ can be interpreted as the probability that the relapse event (first use of drugs after $t = 0$) occurred between t and $t+\mathrm{d}t$. Even though the instantaneous relapse rate does not explicitly depend on history or memory, it depends on $C(t)$ and $M(t)$ which dynamically evolve, implicitly imparting event histories into the current relapse rate. Eq. (1) indicates that if the drug supply is unrestricted ($I(t) = 1$), no cues are present ($C(t) = 0$), and an individual is under a "neutral" mental state ($M(t) = 0$) the rate of relapse is given by a reference baseline $R(t) = R_0$. Negative values of the mental state $M(t) < 0$ increase the relapse rate, conversely $R(t)$ vanishes in the case of a strongly positive mental state $M(t) \gg 1$. An alternative model for $R(t)$ may include a maximal saturated value R_{max}, representing the fastest possible rate of acquiring and consuming drugs and that is attained when $C(t) - M(t)$ surpasses a positive threshold. Finally, the probability of relapsing by time T, $P(T)$, can be written in terms of the survival (against relapse) probability up to time T, $S(T)$ given by

$$S(T) = e^{-\int_0^T R(t)\mathrm{d}t}, \quad P(T) = 1 - S(T). \tag{2}$$

Next, we describe an event-based model for the dynamics of the mental state $M(t)$.

2.2. The PA/NA mental state model

The so-called "Positive Activation, Negative Activation" (PA/NA) model posits that affects arising from positive and negative experiences are not coupled [39–41] and might be processed on different neural substrates [42,43]. Thus a realistic representation of the mental state $M(t)$ is as a sum of two contributions, $M(t) = M_a(t) + M_b(t)$, where positive events affect $M_a(t)$, negative ones affect $M_b(t)$, and the two evolve independently. Negative events, or stressors, are known to impact one's mental state more than positive ones, a neurological phenomenon known as the "negativity bias" [44]; recent studies also show that stressors tend to affect drug users more than the general population [45,46], and that drug abuse produces hypersensitivity to negative emotional distress [25,47,48]. Note that the exponential term $e^{-M(t)}$ in Eq. (1) weights negative mental states more than positive ones, in accordance with negativity bias [44]. We model the dynamics of M_a and M_b using different processing rates $\kappa_a(t)$ and $\kappa_b(t)$ as

$$\frac{\mathrm{d}M_a}{\mathrm{d}t} = -\kappa_a(t)M_a + \sum_{i,t \geq t_i^a} A_i \delta(t - t_i^a), \tag{3a}$$

$$\frac{\mathrm{d}M_b}{\mathrm{d}t} = -\kappa_b(t)M_b - \sum_{j,t \geq t_j^b} B_j \delta(t - t_j^b). \tag{3b}$$

In Eq. (3a) $A_i > 0$ is the intensity of positive life event i, as experienced by the individual in recovery, occurring at time t_i^a and $\kappa_a(t) > 0$ is the processing rate that returns $M_a(t)$ to steady state. Similarly for $-B_j < 0$, t_j^b and $\kappa_b(t)$ in Eq. (3b). Since M_a and M_b are decoupled and $\kappa_a(t) \neq \kappa_b(t)$, Eqs. (3a) and (3b) are our mathematical representation of the PA/NA model. We solve them assuming that there are no initial affects, $M_a(t = 0) = M_b(t = 0) = 0$ and that $\kappa_a(t) = \kappa_a$ and $\kappa_b(t) = \kappa_b$ are time-independent. Non-zero initial affects can be incorporated by setting $A_1 = M_a(t = 0)$ at $t_{i=1}^a = 0$ or $B_1 = -M_b(t = 0)$ at $t_{j=1}^b = 0$ in the sequence of positive or negative life events. Time-dependent $\kappa_a(t), \kappa_b(t)$ are discussed in the Appendix. We solve Eqs. (3a) and (3b) under the above approximations to find

$$M_a(t) = \sum_{i,t \geq t_i^a} A_i e^{-\kappa_a(t-t_i^a)}, \qquad M_b(t) = \sum_{j,t \geq t_j^b} B_j e^{-\kappa_b(t-t_j^b)}. \tag{4}$$

The mental state integrated up to time T after n_a positive and n_b negative life events, such that $t_{n_a}^a \leq T \leq t_{n_a+1}^a$ and $t_{n_b}^b \leq T \leq t_{n_b+1}^b$, is thus given by

$$\int_0^T M(t)\mathrm{d}t = \int_0^T \left(M_a(t) + M_b(t)\right)\mathrm{d}t$$
$$= \frac{1}{\kappa_a} \sum_{i=1}^{n_a} A_i \left(1 - e^{-\kappa_a(T-t_i^a)}\right) - \frac{1}{\kappa_b} \sum_{j=0}^{n_b} B_j \left(1 - e^{-\kappa_b(T-t_j^b)}\right). \tag{5}$$

The effects of a sequence of n_a events defined by $\{A_i, t_i^a\}$ on the integrated mental state in Eq. (5) can be reproduced by a single event of amplitude Z_a at specific time t_a

$$Z_a = \sum_{i=1}^{n_a} A_i, \quad t_a = \frac{1}{\kappa_a} \ln \left[\frac{\sum_{i=1}^{n_a} A_i e^{\kappa_a t_i^a}}{\sum_{i=1}^{n_a} A_i} \right]. \tag{6}$$

Similarly, a sequence of n_b events $\{-B_j, t_j^b\}$ generates an integrated mood that can be reproduced by single event

$$Z_b = \sum_{j=1}^{n_b} B_j, \quad t_b = \frac{1}{\kappa_b} \ln \left[\frac{\sum_{j=0}^{n_b} B_j e^{\kappa_b t_j^b}}{\sum_{i=0}^{n_b} B_j} \right]. \tag{7}$$

Thus far, we have modeled the dynamics of positive and negative mental state variables. Included in the relapse rate $R(t)$ is also a dependence on random cues that trigger the memory of drug-induced euphoria. The model for cues shares many features of the negative mood variable and is described below.

Table 1

Relevant quantities and parameter ranges for the relapse models presented in Eqs. (1), (3a), (3b) (distinct mental state neurocircuitry for few positive and negative events, no cues); Eqs. (1), (19), (common mental state neurocircuitry for random, Gaussian distributed positive and negative events, no cues); Eqs. (1), (9), (36), (37) (distinct mental state neurocircuitry for uniform, positive events, subject to Poisson distributed drug-related cues) and time-dependent forms for the processing rates.

Symbol	Quantity	Range
M_a	positive activity of the mental state	~ 10
M_b	negative activity of the mental state	~ -10
C	mental response to cues	~ 1
$\kappa_a,\ \kappa_b$	equilibration values of the mental state processing rates	$\sim 1/\text{day}$
$\kappa_{a,0},\ \kappa_{b,0}$	onset values of the mental state processing rates	$0.6 \sim 0.8\kappa_{a,b}$ [49]
$\gamma_a,\ \gamma_b$	recovery rates for $\kappa_a(t)$ and $\kappa_b(t)$	$0.002 \sim 0.02/\text{day}$ [49]
κ_c	processing rates of drug-related cues and memories	$\sim 10/\text{day}$
R_0	rate of relapse in the neutral mental state (without inputs)	$\sim 10^{-3}/\text{day}$
A_i	intensity of positive life event i	~ 1
B_j	intensity of negative life event j	~ 1
w_{peak}	intensity of most pleasurable drug-taking reward response	~ 1
t_i^a	time of occurrence of positive life event i	$\sim \text{day}$
t_j^b	time of occurrence of negative life event j	$\sim \text{day}$
t_ℓ^q	time of occurrence of cue ℓ	$\sim \text{day}$
λ_q	Poisson process rate for the occurrence of cues	$\sim 1/\text{day}$
Y	continuous input to the mental state	
κ	mental state processing rate for $\kappa_a = \kappa_b$	
λ	Gaussian noise intensity in the OU process for the mental state	

2.3. External cues

Here we discuss representations for $C(t) \geq 0$. External cues can trigger memories of the pleasurable feelings associated with drug taking [50,51]. We model these memories as impulses occurring at times t_ℓ^c whose effects decay with rate κ_c. Thus, the dynamics of $C(t)$, the overall motivation from cues, is given by

$$\frac{dC}{dt} = -\kappa_c(t)C + \sum_{\ell, t \geq t_\ell^c} C_\ell \delta(t - t_\ell^c). \tag{8}$$

The amplitude C_ℓ represents the mnemonic strength of a given cue. By the peak-end rule, we assume that the most intense memory is proportional to $w_{\text{peak}} > 0$, the largest reward response during addiction, and set $C_\ell = w_{\text{peak}}$ for all ℓ. We also assume the decay rate $\kappa_c(t)$ associated with the permanence of the cue in one's memory is a constant, $\kappa_c(t) = \kappa_c$, and that there are no initial cues, $C(t = 0) = 0$, which leads to

$$C(t) = w_{\text{peak}} \sum_{\ell, t \geq t_\ell^c} e^{-\kappa_c(t - t_\ell^c)}. \tag{9}$$

3. Results

We now study how external stimuli and intrinsic traits affect the relapse probability $P(T)$. External factors include specific realizations of the $\{A_i, t_i^a\}$ and $\{-B_j, t_j^b\}$ sequences, cue occurrence times $\{t_\ell^c\}$ and drug availability profile $I(t)$. The intrinsic characteristics of an individual include how his or her mental state is affected by stressors, joyous events, and cues, the processing rates for positive and negative events, κ_a and κ_b, for cues, κ_c, and the intensity of the first high w_{peak}. Relevant parameter ranges are listed in Table 1. Specifically, we measure time in units of days and fix $R_0 = 10^{-3}/\text{day}$ consistent with known relapse rates of roughly 40 to 60 percent among opioid abuse disorder patients one year after treatment [52]. We assume drugs are always available and set $I(t) = 1$ throughout the remainder of this work. Relapse is not possible if drugs are not available.

3.1. Dynamics without cues

We begin by studying the case of no cues and an unimpeded drug supply so that $C(t) = 0$ and $I(t) = 1$. We first analyze the simple case of a single life event and later consider sequences of multiple negative and positive ones. Our goal is to identify which combination of events (intensity and timing) leads to the smallest relapse likelihood.

3.1.1. Longer-lasting stressors increase the relapse probability; longer-lasting positive events decrease it

We consider a single stressor that is processed at three different rates κ_b. Fig. 1 shows that the longer the stressor affects one's mental state (*i.e.* the lower κ_b), the larger the relapse probability $P(T)$. Corresponding results are shown for a positive experience processed at various rates κ_a: lower values of κ_a result in smaller relapse likelihoods, as the effects of the positive event are retained for a longer time. Due to the exponential term in the relapse rate, stressors result in higher relapse likelihoods compared to positive ones of the same amplitude.

3.1.2. Clustered stressors increase the relapse probability more than disperse ones

We now include multiple life events and study how their timing affects the likelihood of relapse. Let us start with two negative events, $\{-B_1, t_1^b\}$ and $\{-B_2, t_2^b\}$, that define the time interval $\Delta_b = t_2^b - t_1^b \geq 0$. We then define the effective time $U(T)$ given by

$$U(T) \equiv -\frac{\ln S(T)}{R_0} = \int_0^T e^{-M(s)} ds$$
$$= t_1^b + \int_0^{\Delta_b} e^{B_1 e^{-\kappa_b s}} ds + \int_{\Delta_b}^{T - t_1^b} e^{\left(B_1 + B_2 e^{\kappa_b \Delta_b}\right) e^{-\kappa_b s}} ds. \tag{10}$$

If $B_1, B_2 = 0$ (as in the "neutral" case or baseline) Eq. (10) gives $U(T) = T$; finite values of B_1, B_2 lead to $U(T) > T$, increasing the relapse probability $P(T) = 1 - S(T)$ above that of the baseline.

We now consider the family of paired events where the amplitudes B_1, B_2 are fixed and where t_1^b, t_2^b are chosen such that for $T > t_2^b$ the two events yield the same integrated mood as the single event $\{Z_b, t_b\}$ defined in Eq. (7). This implies that $B_1 e^{\kappa_b t_1^b} + B_2 e^{\kappa_b t_2^b} \equiv H_b$ must be a constant, leaving one degree of freedom, which we choose to be Δ_b. The above constraints also impose that the integrated mental state, $\int_0^T M(s) ds$ is invariant for all paired events within the family defined by B_1, B_2, H_b. We may now ask: within this family of paired events, where
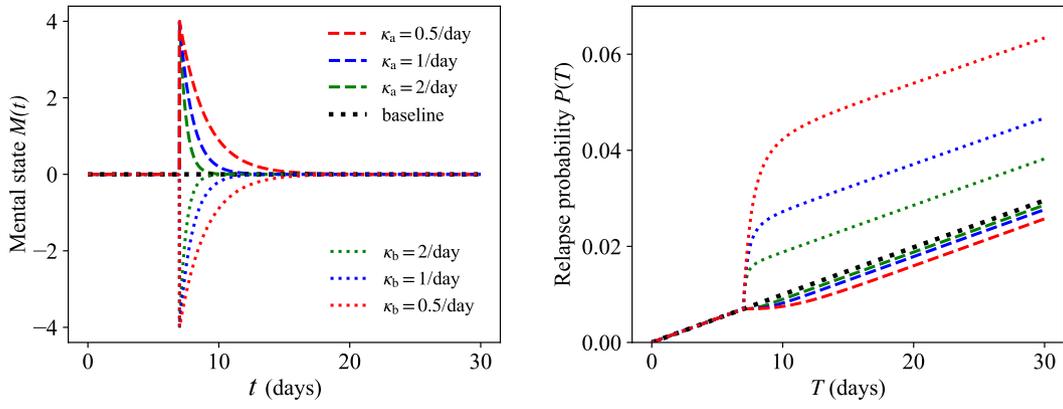
Fig. 1. Mental state at time t, $M(t)$, and the probability of relapse before time T, $P(T)$, upon exposure to a single stressor $\{-B_1, t_1^b\}$ or to a single positive event $\{A_1, t_1^a\}$ for three processing rates κ_b or $\kappa_a = 2, 1, 0.5$/day with $B_1 = A_1 = 4$, $t_1^b, t_1^a = 7$ days, $R_0 = 10^{-3}$/day, $M_0 = 0$. The relapse probability decreases with κ_b so that the longer a stressor impacts one's mental state, the larger the likelihood of relapse. The opposite is true for positive events, for which the longer memory of a positive event is retained, the less likely relapse is. Note the more pronounced effect of the negative mental state B_1, compared to the positive one A_1 under the same processing rate despite their amplitudes being the same. The mental state $M(t) = M_a(t) + M_b(t)$ is given by Eqs. (4); the relapse probability $P(T)$ by Eqs. (1) and (2).
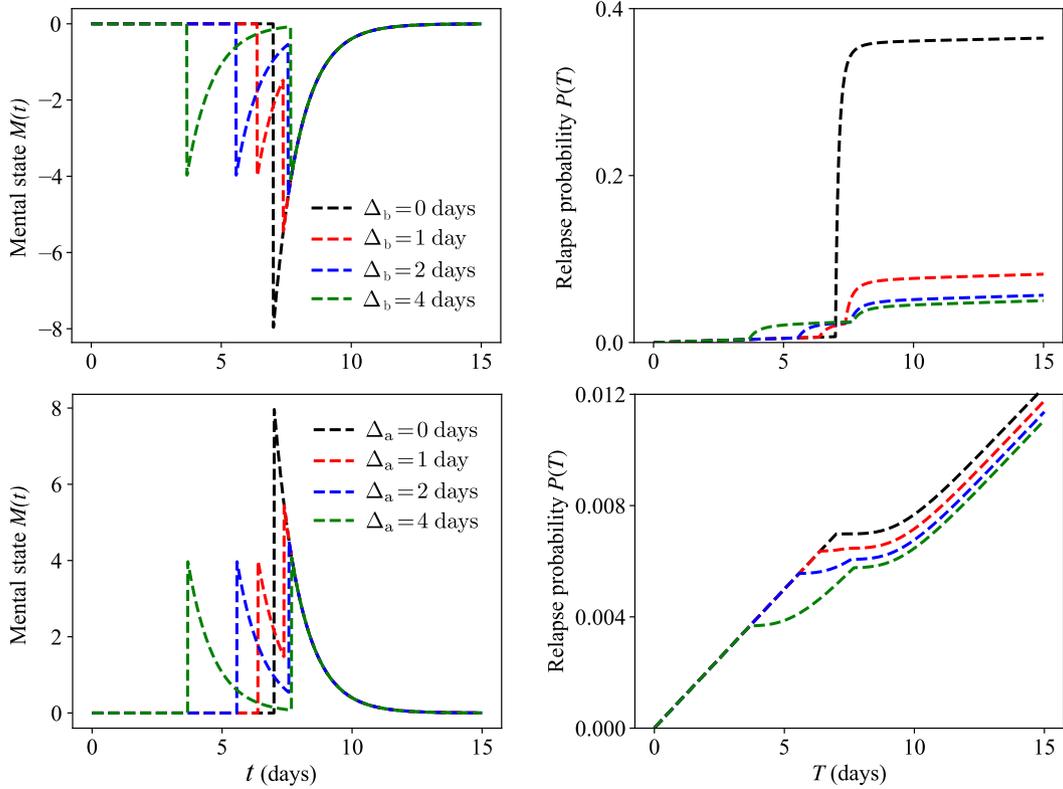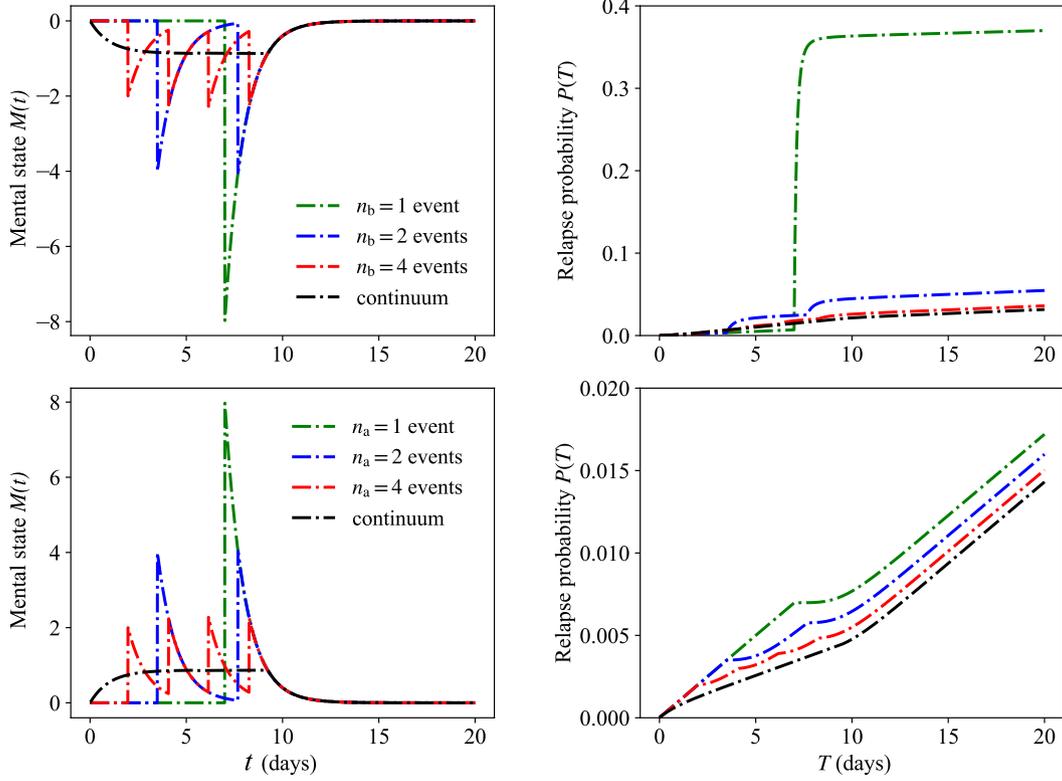

Fig. 2. Top row: Mental state $M(t)$ and relapse probability $P(T)$ upon exposure to two stressors $\{-B_1, t_1^b\}$ and $\{-B_2, t_2^b\}$ separated by lag times $\Delta_b = t_2^b - t_1^b = 0, 1, 2, 4$ days and obtained using Eqs. (1), (2), (4), and (12). Parameters are $\kappa_b = 1$/day, $B_1 = B_2 = 4$, $R_0 = 10^{-3}$/day, $M_0 = 0$. All stressor pairs define the same integrated mental state defined in Eq. (5) and are equivalent to the single event $\{-Z_b, t_b\}$ shown in the red curve. For each Δ_b, the corresponding t_1^b is derived from the constraint $H_b = B_1 e^{\kappa_b t_1^b} + B_2 e^{\kappa_b (t_1^b + \Delta_b)}$ where $H_b = Z_b e^{\kappa_b t_b}$, $Z_b = (B_1 + B_2)$, and $t_b = 7$ days. Notice that $P(T)$ decreases with Δ_b, implying that stressors should be as spaced apart as possible to decrease the likelihood of relapse in accordance with our analytical findings. Bottom row: Corresponding plots for two positive events, $\{A_1, t_1^a\}$ and $\{A_2, t_2^a\}$ separated by lag times $\Delta_a = t_2^a - t_1^a = 0, 1, 2, 4$ days with $A_1 = A_2 = 4$ and all other parameters the same as above. The constraint can be obtained by setting a → b in the two-stressor constraint expression, with $t_a = 7$ days. Here, $P(T)$ decreases with Δ_a, implying that the best protection against relapse is by experiencing well-spaced positive events rather than large clustered ones. Small, repeated joys and small, repeated unpleasant events are better than large a jolt of happiness or catastrophe.

the integrated mental state is fixed, which choice of Δ_b minimizes the relapse probability at any time $T > t_2^b$? We first express t_1^b in terms of H_b and Δ_b,

$$t_1^b = \frac{1}{\kappa_b} \ln\left(\frac{H_b}{B_1 + B_2 e^{\kappa_b \Delta_b}}\right), \tag{11}$$

and make the dependence of $U(T)$ on Δ_b explicit so that $U(T) \to U(T; \Delta_b)$ and

$$\kappa_b U(T; \Delta_b) = \ln\left(\frac{H_b}{B_1 + B_2 e^{\kappa_b \Delta_b}}\right)$$
$$+ \text{Ei}(B_1) - \text{Ei}(B_1 e^{-\kappa_b \Delta_b})$$
$$+ \text{Ei}(B_1 e^{-\kappa_b \Delta_b} + B_2) - \text{Ei}(H_b e^{-\kappa_b T}), \tag{12}$$

Fig. 3. Top row: Mental state $M(t)$ and relapse probability $P(T)$ upon exposure to $n_b = 1, 2, 4$ negative events $\{-B_i, t_i^b\}$ and a continuum of stressors. All curves are obtained using Eqs. (1), (2), (4), and (12). Sequences define the same integrated mental state defined in Eq. (5) and are equivalent to the single event $\{-Z_b, t_b\}$ shown in the red curve, where $Z_b = 8$ and $t_b = 7$ days. Within each sequence, events carry the same amplitude B_i and are separated by the same time interval $\Delta_b = 3.5$ days ($n_b = 2$, black curve), 2 days ($n_b = 4$, blue curve), and 0.1 days (continuum, green curve). Other parameters are $\kappa_b = 1/\text{day}$, $R_0 = 10^{-3}/\text{day}$, $M_0 = 0$. Bottom row: Corresponding plots for sequences of equivalent positive events with $Z_a = 8$ and $t_a = 7$ days with $\kappa_a = 1/\text{day}$ and $\Delta_a = 3.5$ days ($n_a = 2$, black curve), 2 days ($n_a = 4$, blue curve), and 0.1 days (continuum, green curve). Notice that for both positive and negative events the relapse probability is lowest for small events of limited magnitude.

where the exponential integral $\text{Ei}(x) \equiv \int_{-\infty}^{x} t^{-1} e^t \, dt$. Since B_1, B_2, H_b are fixed, the extrema of $U(T; \Delta_b)$ with respect to Δ_b at any time T are given by the zeros of

$$\kappa_b \frac{\partial U(T; \Delta_b)}{\partial \Delta_b} = (1 - B_2) e^{B_1 e^{-\kappa_b \Delta_b}} + \frac{e^{B_2} e^{B_1 e^{-\kappa_b \Delta_b}} - 1}{1 + \frac{B_1}{B_2} e^{-\kappa_b \Delta_b}}. \tag{13}$$

Regardless of B_1, B_2, κ_b, the left hand side of Eq. (13) is a negative function of Δ_b, implying that $U(T; \Delta_b)$ has a maximum at $\Delta_b \to 0$. Since $P(T) = 1 - S(T) = 1 - e^{-R_0 U(T; \Delta_b)}$, we conclude that the largest relapse probability also occurs at $\Delta_b \to 0$; that is, the relapse likelihood is largest when the two negative events occur simultaneously. In the top row of Fig. 2 we show the relapse probability $P(T)$ upon exposure to pairs of stressors that belong to the same family of events with fixed B_1, B_2, H_b and different timings Δ_b. The relapse probability is indeed largest when the time lag between the two stressors is smallest, $\Delta_b \to 0$. We can apply the same arguments to more than two events and show that as the number of stressors increases, so does the likelihood of relapse. Given a negative integrated mental state generated by a set of n_b negative events occurring within time T, the relapse likelihood is largest when stressors are coincident, and is reduced when stressors are spread out. Fig. 3 shows the relapse probability for $n_b = 1, 2, 4$ and a continuum of negative events. In our model, relapse after a single catastrophic event is more likely than after a series of smaller stressors which cumulatively yield the same integrated negative mental state as the single catastrophic stressor.

3.1.3. Dispersed positive events decrease the relapse probability more than clustered ones

We can derive similar expressions to Eq. (10) for two positive life events for which the corresponding $U(T)$ is obtained by substituting

$B_{1,2} \to -A_{1,2}$, and $t_1^b, \Delta_b, \kappa_b \to t_1^a, \Delta_a, \kappa_a$, respectively. Using the same methods as for pairs of negative events, we can show that the occurrence of two positive events decreases the likelihood of relapse the most when the two positive events are well spaced out. Results are shown in the bottom row of Fig. 2 for pairs of positive events with fixed A_1, A_2, H_a and different timings. The smallest likelihood of relapse occurs when the time lag between positive events Δ_a is large, conversely, the likelihood of relapse is most pronounced for $\Delta_a \to 0$. In the case of multiple, positive life events, as with the findings described for negative life events, the likelihood of relapse decreases the most when an individual experiences many distributed but moderately happy events, compared to a much larger but isolated positive episode that carries the same overall impact as the distributed ones. Results for sequences of multiple events belonging to the same family are shown in the bottom row of Fig. 3 for $n_a = 1, 2, 4$ where events are equally spaced and for a continuum of episodes. As expected, the lowest relapse probability occurs for a uniform distribution of positive events. A modest but continuous source of support is more protective against relapse than a very intense yet short-lived positive experience.

3.1.4. Relapse is least likely if a positive experience occurs immediately after a stressor

We now examine the case of a stressor $\{-B_1, t_1^b\}$ followed by a positive event $\{A_2, t_2^a\}$, where $t_2^a > t_1^b$. We label the positive event A_2 rather than A_1 so that it is clear that the positive event occurs after the negative one. Given an integrated mental state $\int_0^T M(t') \, dt'$ and values for B_1, A_2, the goal is to establish the lag time between the two events that minimizes the likelihood of relapse. The general case of different processing rates $\kappa_a \neq \kappa_b$ does not allow for easy generalization, so we set $\kappa_a = \kappa_b = \kappa$ to simplify our analysis. We write $U(T) = -\ln S(T)/R_0$
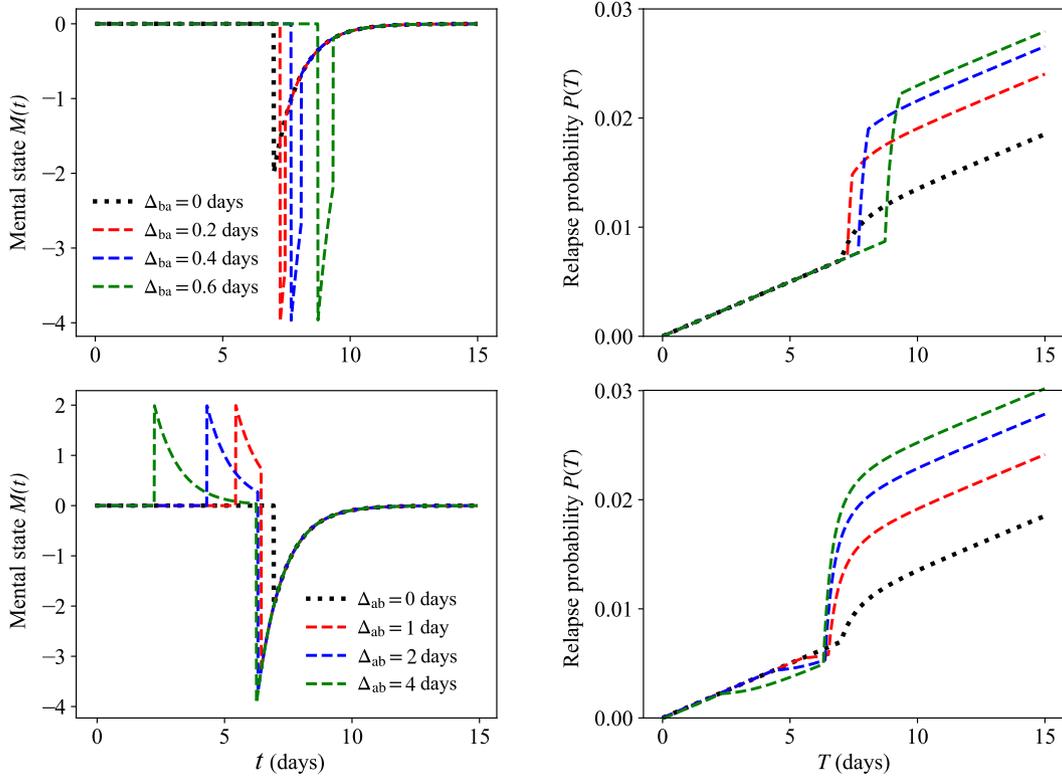
Fig. 4. Top row: Mental state $M(t)$ and relapse probability $P(T)$ upon exposure to a stressor $\{-B_1, t_1^b\}$ followed by a positive event $\{A_2, t_2^a\}$. The two events are separated by lag times $\Delta_{ba} = t_2^a - t_1^b = 0, 0.2, 0.4, 0.6$ hours. All curves are obtained using Eqs. (1), (2), (4), and (14). Parameters are $\kappa_b = \kappa_a = \kappa = 1/\text{day}$, $B_1 = 4$, $A_2 = 2$, $R_0 = 10^{-3}/\text{day}$, $M_0 = 0$ and by setting $H = 2e^7$. All event pairs define the same integrated mental state defined in Eq. (5) for $T > t_2^a$. Notice that $P(T)$ increases with Δ_{ba}, implying that given a stressor, the likelihood of relapse is lowest the earlier a counteracting positive event occurs, in accordance with our analytical findings. Bottom row: Corresponding plots for a positive event $\{A_1, t_1^a\}$ followed by a stressor $\{-B_2, t_2^b\}$ with lag times $\Delta_{ab} = t_2^b - t_1^a = 0, 1, 2, 4$ days with $A_1 = 2$, $B_2 = 4$ and all other parameters are the same as above. Here, $P(T)$ also increases with Δ_{ab} and is smallest for $\Delta_{ab} \to 0$.

in terms of $\Delta_{ba} = t_2^a - t_1^b$ and make the dependence on Δ_{ba} explicit in the expression for $U(T; \Delta_{ba})$ as follows

$$
\kappa U(T; \Delta_{ba}) = \ln\left(\frac{H}{B_1 - A_2 e^{\kappa \Delta_{ba}}}\right)
$$
$$
+ \text{Ei}(B_1) - \text{Ei}(B_1 e^{-\kappa \Delta_{ba}}) \tag{14}
$$
$$
+ \text{Ei}(B_1 e^{-\kappa \Delta_{ba}} - A_2) - \text{Ei}(He^{-\kappa T}),
$$

where $H \equiv B_1 e^{\kappa t_1^b} - A_2 e^{\kappa t_1^a}$ is a constant that ensures $\int_0^T M(t') dt'$ is independent of Δ_{ba}. We can thus write

$$
\kappa \frac{\partial U(T; \Delta_{ba})}{\partial \Delta_{ba}} = A_2 e^{B_1 e^{-\kappa \Delta_{ba}}} \left(\frac{1 - e^{-\kappa A_2}}{A_2} + \frac{e^{-B_1 e^{-\kappa \Delta_{ba}} - e^{-\kappa A_2}}}{B_1 e^{-\kappa \Delta_{ba}} - A_2}\right). \tag{15}
$$

The left hand side of Eq. (15) is a positive function of Δ_{ba} regardless of A_1, B_2, κ; as a consequence, for $T > t_2^a$, $U(T; \Delta_{ba})$ is an increasing function of Δ_{ba} and attains its lowest value at $\Delta_{ba} = 0$. Thus, the relapse probability is also the lowest for $\Delta_{ba} = 0$. Once a negative life event occurs, the way to minimize the occurrence of relapses is for the individual to experience a healing, positive experience as soon as possible. Similar results hold in the case of a positive event $\{A_1, t_1^a\}$ followed by a negative event $\{B_2, t_2^b\}$; the relapse probability is lowest when the time lag between the two events is shortest.

In Fig. 4 we show the relapse probability for equivalent pairs of events $\{-B_1, t_1^b\}$ and $\{A_2, t_2^a\}$ that define a fixed $H \equiv B_1 e^{\kappa t_1^b} - A_2 e^{\kappa t_2^a}$ for $\kappa_a = \kappa_b = \kappa$. For large enough T, $P(T)$ decreases with Δ_{ba}, confirming our analytic predictions. The same finding arises for equivalent pairs of events $\{A_1, t_1^a\}$ and $\{-B_2, t_2^b\}$ that define a fixed $H \equiv -A_1 e^{\kappa t_1^a} + B_2 e^{\kappa t_2^b}$ for $\kappa_a = \kappa_b = \kappa$. To derive the mathematical results presented for pairs of events of amplitude (A_1, A_2), (B_1, B_2), (B_1, A_2) and (A_1, B_2) we assumed

that no other prior events occurred; however, it is possible to show that our findings remain valid in the presence of earlier events. For example, given the events $\{A_1, t_1^a\}$, $\{-B_2, t_2^b\}$, $\{-B_3, t_3^b\}$ with $t_3^b \geq t_2^b \geq t_1^a$ processed at the same rate $\kappa_a = \kappa_b = \kappa$ one can show that the relapse probability is still maximized upon clustering the two negative events (B_2, B_3) and setting $\Delta_b = t_3^b - t_2^b \to 0$.

We now consider the general case $\kappa_a \neq \kappa_b$. In Fig. 5 we show results for pairs of events $\{A_1, t_1^a\}$ and $\{-B_2, t_2^b\}$ where $A_1 = B_2$ and $\Delta_{ab} \equiv t_2^b - t_1^a$, and for pairs of events $\{-B_1, t_1^b\}$ and $\{A_2, t_2^a\}$ where $B_1 = A_2$ and $\Delta_{ba} \equiv t_2^a - t_1^b$. The long-term relapse probability $P(T)$ is largely insensitive to the absolute timing of the pair of events, as long as $T - t_2^{a,b} \gg \kappa_a^{-1}, \kappa_b^{-1}$; however, it strongly depends on the event order and the magnitude of the time lag Δ_{ab} or Δ_{ba}. For a fixed $\Delta_{ab} = \Delta_{ba}$, $P(T)$ may depend significantly on the order of events. In general, the larger $\kappa_a \Delta_{ab}$ and $\kappa_b \Delta_{ba}$, the less sensitive the relapse probability is to the order of events as shown by comparing the cases $\Delta_{ab} = \Delta_{ba} = 4$ days with $\Delta_{ab} = \Delta_{ba} = 1$ day in Fig. 5. Note that since $\kappa_a \neq \kappa_b$ it is impossible for the pairs of events in Fig. 5 to define the same integrated mental state $\int_0^T M(t') dt'$ for any given T.

Finally, given a stressor $\{-B_1, t_1^b\}$ which is processed at a rate κ_b we determine which later event $\{A_2, t_2^a\}$ processed at rate κ_a will yield the same relapse probability as the baseline case, where no events occur. To do this, we note that under the baseline, $U(T) = T$ and that since it is not possible to define a single event as in Eq. (14) for $\kappa_a \neq \kappa_b$, we must write $U(T; \Delta_{ba})$ in its general form

$$
U(T; \Delta_{ba}) = t_1^b + \int_0^{\Delta_{ba}} e^{B_1 e^{-\kappa_b t}} dt + \int_{\Delta_{ba}}^{T - t_1^b} e^{B_1 e^{-\kappa_b t'} - A_2 e^{-\kappa_a(t' - \Delta_{ba})}} dt', \tag{16}
$$
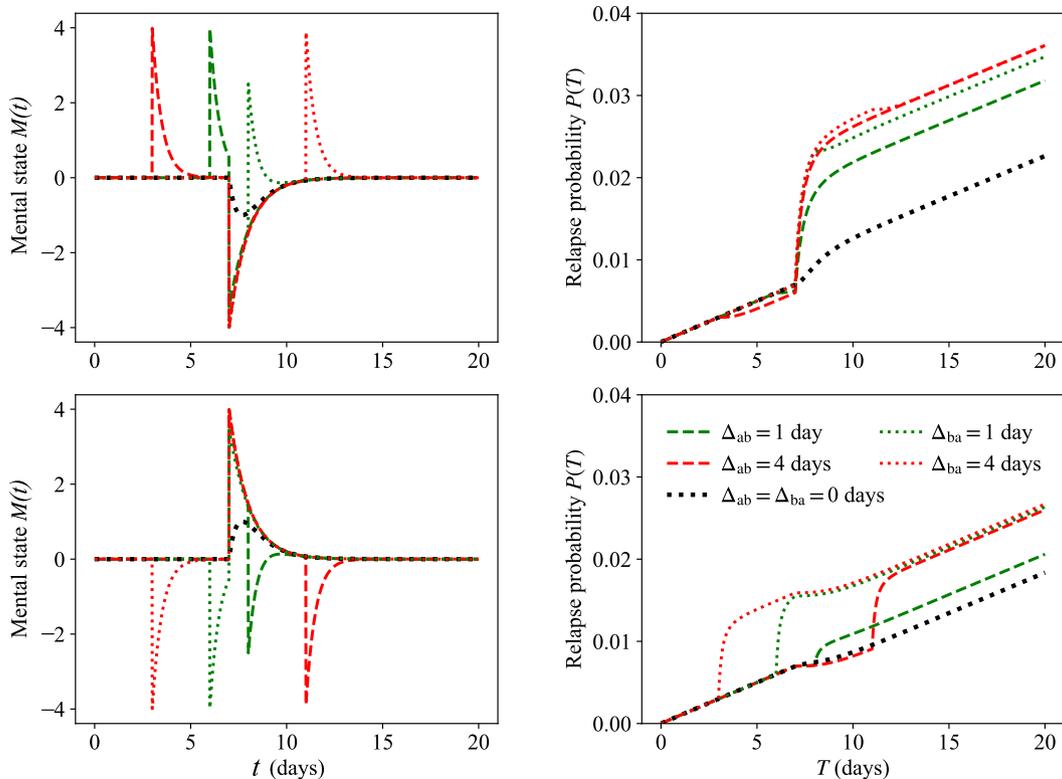
Fig. 5. Top row: Mental state $M(t)$ and relapse probability $P(T)$ upon exposure to two events of opposite sign $\{A_i, t_i^a\}$ and $\{-B_j, t_j^b\}$ for $\kappa_a = 2$/day and $\kappa_b = 1$/day where $i = 1, j = 2$ or $j = 1, i = 2$. All curves are obtained using Eqs. (1), (2), (4), and (14). Events carry the amplitudes $A_i = B_j = 4$; the other parameters are set at $M_0 = 0, R_0 = 10^{-3}$. Lag times are evaluated by setting $t_j^b = 7$ days where $j = 1$ for lag times $\Delta_{ba} = t_2^a - t_1^b$ and $j = 2$ for lag times $\Delta_{ab} = t_1^b - t_1^a$. For large enough $\Delta_{ab} = \Delta_{ba} = 4$ days the relapse probability is independent of the order of events; however, for smaller lag times $\Delta_{ab} = \Delta_{ba} = 1$ day, the order of events matters and the relapse probability is lower when the positive event $\{A_1, t_1^a\}$ occurs prior to the stressor $\{-B_2, t_2^a\}$. If the two events are concurrent and $\Delta_{ab} = \Delta_{ba} = 0$ the total input to the mental state is negative since $\kappa_b < \kappa_a$ and the effects of the stressor are retained for a longer time than those of the positive event. Bottom row: Corresponding plots for $\kappa_a = 1$/day and $\kappa_b = 2$/day with all other parameters and events same as those of the top row, and where the ordering of positive and negative events is reversed. Here, the order of events plays an even more crucial role when the time lag $\Delta_{ab} = \Delta_{ba} = 1$ as the relapse probability is much lower when the positive event $\{A_1, t_1^a\}$ occurs prior to the stressor $\{-B_2, t_2^a\}$. Since $\kappa_b \neq \kappa_a$ it is not possible for the pairs of events to define the same mental state for all values of t.
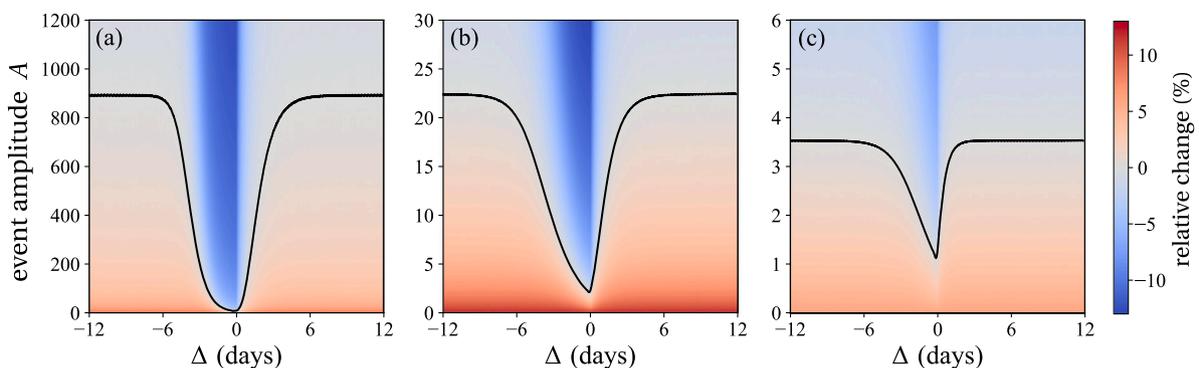
Fig. 6. Long-term percentage changes in the relapse probability after one negative and one positive event relative to the neutral scenario of no events occurring. For $\Delta = \Delta_{ba} = t_2^a - t_1^b > 0$, the stressor $\{-B_1, t_1^b\}$ is followed by a positive event $\{A_2, t_2^a\}$ where $B_1 = 2$, $t_1^b = 12$ days and $A = A_2$ is determined from Eq. (17) at $T = 30$ days. The color shading represents the percentage change of $P(T = 30)$ assuming the two events have occurred relative to the neutral case. The black curve represents the amplitude of A_2 that yields the same relapse probability as the neutral case effectively neutralizing the effects of the stressor. For $\Delta = -\Delta_{ab} = t_1^a - t_2^b < 0$ the positive event $\{A_1, t_1^a\}$ is followed by a stressor $\{-B_2, t_2^b\}$ where $B_2 = 2$, $t_2^b = 12$ days. Here, the black curve tracks the amplitude of a preemptive positive event A_1 that would neutralize the future $B_2 = 2$ stressor at $T = 30$ days as determined from Eq. (17). In panel (a) we set $\kappa_a = 2$/day, $\kappa_b = 1$/day; in panel (b) we set $\kappa_a = \kappa_b = 1$/day; and in panel (c) we set $\kappa_a = 1$/day, $\kappa_b = 2$/day. The asymmetry between the positive and negative values of Δ underlines the importance of event order. For a given $\Delta = \Delta_{ba} > 0$, the value of A_2 necessary to balance $B_1 = 2$ is larger than the value of A_1 necessary to balance $B_2 = 2$ when $\Delta = -\Delta_{ab} = -|\Delta_{ba}| < 0$. Upon comparing the black lines in the three panels for fixed $\Delta = \Delta_{ba} > 0$ the value of A_2 necessary to neutralize the B_1 stressor is larger when κ_a is larger or κ_b is lower, i.e. under fast processing of positive events or longer-lasting stressors. Similar considerations apply when $\Delta = \Delta_{ab} < 0$.

where $\Delta_{\text{ba}} = t_2^{\text{a}} - t_1^{\text{b}}$. To find the value of A_2 that balances $U(T; \Delta_{\text{ba}})$ with the baseline $U(T) = T$, we must solve

$$U(T; \Delta_{\text{ba}}) = t_1^{\text{b}} + \frac{1}{\kappa_{\text{b}}} \left[\text{Ei}(B_1) - \text{Ei}\left(B_1 e^{-\kappa_{\text{b}} \Delta_{\text{ba}}}\right) \right]$$
$$+ \frac{1}{\kappa_{\text{a}}} \left[\text{Ei}(-A_2) - \text{Ei}\left(-A_2 e^{-\kappa_{\text{a}}(T - t_1^{\text{b}} - \Delta_{\text{ba}})}\right) \right] \quad (17)$$
$$= U(T) = T.$$

Under the assumption $\kappa_{\text{a}} \Delta_{\text{ba}}, \kappa_{\text{b}} \Delta_{\text{ba}} \gg 1$, and using the identity $\lim_{x \to 0} \text{Ei}(x) = \ln|x| + \gamma$, where γ is the Euler–Mascheroni constant, Eq. (17) can be simplified to

$$\text{Ei}(-A_2) - \gamma - \ln(A_2) = \frac{\kappa_{\text{a}}}{\kappa_{\text{b}}} \left[\ln(B_1) + \gamma - \text{Ei}(B_1) \right]. \quad (18)$$

Eq. (18) yields the value of A_2 that neutralizes the effects of a stressor of amplitude B_1 so that at long times the relapse rate is the same as if neither event occurred. It is straightforward to show that upon substituting $B_1 \to -A_1$ and $A_2 \to -B_1$ Eq. (18) still holds when the order of events is reversed and the positive event occurs prior to the negative one. The black curves in Fig. 6 trace the values of $A = A_2$ that balance a stressor of amplitude B_1 given a lag time $\Delta = \Delta_{\text{ba}} > 0$ for various choices of κ_{a} and κ_{b}. These results correspond to positive values of Δ. *Vice-versa*, the amplitude of a protective event $A = A_1$ that can balance a later stressor of amplitude B_2 are shown for negative values of $\Delta = -\Delta_{\text{ab}} < 0$. The asymmetry between positive and negative values of Δ for all choices of κ_{a} and κ_{b} implies that a modest amplitude of the positive event is required to balance a fixed stressor, regardless of whether the positive event occurs before or after the stressor. The other color-coded regions in Fig. 6 show the percent increase (or decrease) of the relapse probability $P(T)$ compared to the neutral case of no negative or positive life event, for specific values of $A_1, A_2, B_1, B_2, t_1^{\text{a}}, t_1^{\text{b}}, t_2^{\text{a}}, t_2^{\text{b}}, T, \kappa_{\text{a}}, \kappa_{\text{b}}$.

3.1.5. A constant source of positivity can offset the random lows of life

We now study the scenario in which there is a constant input Y to the mental state which may represent a continuous stressor or source of support. We also assume that positive and negative life events occur randomly and are processed at rates $\kappa_{\text{a}} = \kappa_{\text{b}} = \kappa$. Under these assumptions we describe the dynamics for $M = M_{\text{a}} + M_{\text{b}}$ as

$$\frac{\text{d}M}{\text{d}t} = -\kappa M + Y + \xi(t), \quad (19)$$

where $\xi(t)$ is a Gaussian white noise term that represents the random, positive and negative, life events. We set the general initial mental state value $M(t = 0) = M_0$ and write the mean and correlation function of $\xi(t)$ as

$$\langle \xi(t) \rangle = 0,$$
$$\langle \xi(t)\xi(t') \rangle = 2\lambda \delta(t - t'). \quad (20)$$

Eq. (20) defines an Ornstein–Uhlenbeck stochastic process, a classic paradigm in statistical mechanics [53–56]. The relapse rate of the neutral case, where there are no life events or continuous inputs to perturb an individual's mental state and $Y = \xi(t) = 0$, is given by

$$R_{\text{d}}(t) = R_0 e^{-M_0 e^{-\kappa t}}. \quad (21)$$

If $Y \neq 0$ and $\xi(t) \neq 0$, Eq. (19) can be solved as

$$M(t) = \mu_{\text{m}}(t) + \int_0^t e^{-\kappa(t-t')} \xi(t') \text{d}t',$$
$$\mu_{\text{m}}(t) \equiv \frac{Y}{\kappa} + \left(M_0 - \frac{Y}{\kappa}\right) e^{-\kappa t}. \quad (22)$$

Associated with Eqs. (19) and (20) is a Fokker–Planck equation governing the dynamics of the probability density function $P_{\text{m}}(M, t)$ [54,55]

$$\frac{\partial P_{\text{m}}(M, t)}{\partial t} = \frac{\partial}{\partial M}\left((\kappa M - Y)P_{\text{m}}\right) + \lambda \frac{\partial^2 P_{\text{m}}}{\partial M^2}. \quad (23)$$

The solution to Eq. (23) and the initial condition $P(M, t = 0) = \delta(M - M_0)$ is

$$P_{\text{m}}(M, t) = \frac{1}{\sqrt{2\pi\sigma_{\text{m}}^2(t)}} e^{-\frac{(M - \mu_M(t))^2}{2\sigma_{\text{m}}^2(t)}}, \qquad \sigma_{\text{m}}^2(t) \equiv \frac{\lambda}{k}(1 - e^{-2kt}). \quad (24)$$

In the limit $t \to \infty$, Eq. (24) defines a steady state Gaussian distribution centered at Y/κ with variance λ/κ. The expected time-dependent relapse rate is given by

$$\langle R(t) \rangle = R_0 \langle e^{-M(t)} \rangle = R_0 \int_{-\infty}^{\infty} e^{-M} P(M, t) \text{d}M, \quad (25)$$

which is explicitly expressed as

$$\langle R(t) \rangle = R_0 \exp\left[-\mu_{\text{m}}(t) + \frac{1}{2}\sigma_{\text{m}}^2(t)\right], \quad (26a)$$
$$\langle R(t \to \infty) \rangle = R_0 \exp\left[\frac{(\lambda - 2Y)}{2\kappa}\right]. \quad (26b)$$

The relapse rate in Eq. (26b) can be compared with the equivalent expression obtained in the absence of noise, *i.e.* for $Y \neq 0$ and $\xi(t) = \lambda = 0$

$$\frac{\langle R(t \to \infty) \rangle}{R(t \to \infty; \xi(t) = 0)} = e^{\lambda/2\kappa} > 1. \quad (27)$$

Since the above λ-independent ratio is always larger than one, Eq. (27) implies that unbiased noise, where positive and negative life events are equally likely in frequency and magnitude, results in a larger relapse rate than the noise-free case, regardless of the sign of Y. Mathematically, this result stems from the asymmetry in $R_0 e^{-M(t)}$ where the increase due to a stressor is much larger than the decrease following a positive fluctuation of similar amplitude, consistent with the brain's negativity bias [44]. We can also compare the general case $Y \neq 0$ and $\xi(t) \neq 0$ with the neutral case $Y = \xi(t) = 0$ yielding

$$\frac{\langle R(t \to \infty) \rangle}{R_{\text{d}}(t \to \infty)} = \exp\left[\frac{(\lambda - 2Y)}{2\kappa}\right]. \quad (28)$$

The values of Y, λ in Eq. (28) can be tuned so that the driving term and the noise balance each other. Specifically, for the long term expected relapse rate in the presence of noise to be less than the relapse rate in the absence of any external input, the constant input Y must obey $Y > \lambda/2$. Given the form for $P(T)$ in Eq. (2), we can write the expected relapse probability as

$$\langle P(T) \rangle = 1 - \left\langle \exp\left[-R_0 \int_0^T e^{-M(t)} \text{d}t\right] \right\rangle \quad (29)$$

and approximate it in the $\kappa T \gg 1$ limit by

$$\langle P(T) \rangle \approx 1 - \exp\left[-R_0 \int_0^T \langle e^{-M(t)} \rangle \text{d}t\right]$$
$$\approx 1 - \exp\left[-e^{\frac{\lambda - 2Y}{2\kappa}} R_0 T\right]. \quad (30)$$

In the Appendix we discuss Eq. (29) and cases where the approximation in Eq. (30) fails, namely in the $\kappa \to 0$ limit. Fig. 7 shows the expected relapse rate $\langle R(t) \rangle$ as κ, Y, λ are varied. Results derived from 100,000 simulations of the stochastic process in Eq. (19) are compared with predictions from the analytical result (Eq. (26a)). We also show the relapse rate for the baseline given by $R_{\text{d}}(t) = R_0$. The expected relapse rate increases with the noise amplitude λ and decreases with the magnitude of the positive experience Y and with the processing rate κ. Lower κ values imply longer processing times for all events; however, since the asymmetry in $R(t)$ assigns more weight to negative occurrences, a larger likelihood of relapse is observed as $\kappa \to 0$. The corresponding values of the expected relapse probability $\langle P(T) \rangle$ obtained from simulations and from the analytical approximation in Eq. (30) are shown in Fig. 8.

Finally, we evaluate the first passage statistics to a given mental state $M_{\text{th}} < 0$. Although the threshold level value can be arbitrary, we set it to be negative to represent a critically unhappy mental state. The dynamics of the mean first passage time $T_{\text{m}}(M)$ to reach M_{th} starting
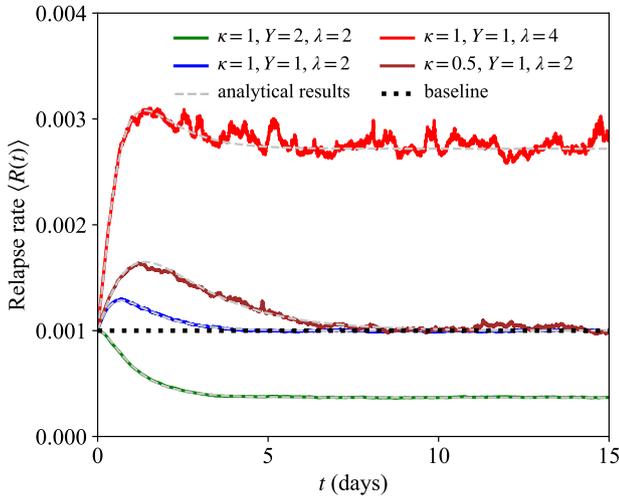
Fig. 7. Dynamics of $\langle R(t) \rangle$ averaged over 100,000 realizations of the Ornstein–Uhlenbeck described by Eq. (19) and the analytical expression for $\langle R(t) \rangle$ in Eq. (26a). Parameters are $M_0 = 0$, $R_0 = 10^{-3}$/day. Values in the legend are in units of /day. For $\lambda = 2Y$ the $t \to \infty$ relapse rate in Eq. (26b) $\langle R(t \to \infty) \rangle = R_0$ matches the neutral case of no exposure to any positive or negative life event.

from a given mental state $M > M_{\text{th}}$ can be derived from the backward Kolmogorov equation associated with Eq. (23)

$$\lambda \frac{d^2 T_{\text{m}}}{dM^2} - (\kappa M - Y) \frac{dT_{\text{m}}}{dM} = -1 \tag{31}$$

along with absorbing boundary conditions $T(M_{\text{th}}) = 0$ and $T_{\text{m}}(M \to \infty) = 0$. Eq. (31) can be solved using standard methods to yield

$$T_{\text{m}}(M) = \frac{\sqrt{\pi}}{\kappa} \int_{\sqrt{\frac{\kappa}{2\lambda}}(M_{\text{th}} - Y/\kappa)}^{\sqrt{\frac{\kappa}{2\lambda}}(M - Y/\kappa)} e^{z^2} \text{erfc}(z) dz, \tag{32}$$

where $\text{erfc}(x)$ is the complementary error function $\text{erfc}(x) = 1 - \text{erf}(x)$. Since the argument of the integrand is a positive, decreasing function of z, Eq. (32) implies that $T_{\text{m}}(M)$ is increasing in Y, M and decreasing in λ, M_{th}. This is to be expected, given that large values of Y, M tend to shift the mental state away from the lower negative threshold M_{th}, and given that large λ values lead to larger fluctuations that are more likely to reach the negative M_{th}. However, $T_{\text{m}}(M)$ is non-monotonic with κ as shown in the top row of Fig. 9. Here we plot $T_{\text{m}}(M = 0)$ as derived from Eq. (32) and denote it as $T_{\text{m}}(M = 0 \to M = M_{\text{th}})$ for clarity. Note that $T_{\text{m}}(M = 0)$ decreases with increasing κ at low values of κ and increases with κ at large κ. To understand this non-monotonicity, note that the mental state M will be restored towards Y/κ within a time frame κ^{-1} after any random fluctuation. As $\kappa \to \infty$, this implies that after each random event, $M \to 0$ very quickly and that cumulative effects of multiple past random events will be very limited. As a result, increasing κ when κ is already large will make reaching M_{th} less likely and thus, the mean first passage time will increase.

On the other hand, when $\kappa \approx 0$, M will grow approximately linearly away from M_{th} driven by the Y input while being subject to noise. Whatever the initial value of M, for large enough values of Y and λ, M will most likely become positive before one, or a sequence of, negative random events will lead it close to M_{th}. Increasing $\kappa > 0$ will now lessen any positive values of M, and thus accelerate reaching the M_{th} threshold. Any negative values of M will instead increase as κ is increased, and this will cause a delay in hitting M_{th}. However, given the negative value of the threshold, excursions in the $M > 0$ space will be much longer than those in the $0 < M < M_{\text{th}}$ space, so that acceleration in reaching M_{th} will dominate. As a result, increasing κ when κ is small will lead to a shorter mean first passage time. This effect will be more pronounced for large values of Y, λ as the excursion to, and permanence in, the $M > 0$ space will be more sustained in

these cases. When Y, λ are small and especially if the initial M value is negative, decreases in $T_{\text{m}}(M)$ as κ is increased for small values of κ will be much less evident, as excursions to the $M > 0$ plane will be rare. An alternate representation of Eq. (32) is given by expanding the integrand via a Taylor series and evaluating the integral, leading to

$$T_{\text{m}}(M) = \frac{\pi}{2\kappa} \text{erfi}(z_{\text{in}}) - \frac{z_{\text{in}}^2}{\kappa} {}_2F_2\left(1, 1; \frac{3}{2}, 2; z_{\text{in}}^2\right) \\ - \frac{\pi}{2\kappa} \text{erfi}(z_{\text{eg}}) + \frac{z_{\text{eg}}^2}{\kappa} {}_2F_2\left(1, 1; \frac{3}{2}, 2; z_{\text{eg}}^2\right), \tag{33}$$

where ${}_2F_2$ is the generalized hypergeometric function and

$$z_{\text{in}} = \sqrt{\frac{\kappa}{2\lambda}}\left(M - \frac{Y}{\kappa}\right), \quad z_{\text{eg}} = \sqrt{\frac{\kappa}{2\lambda}}\left(M_{\text{th}} - \frac{Y}{\kappa}\right). \tag{34}$$

Eqs. (32) and (33) are the mean time $T_{\text{m}}(M)$ for an initial mental state M to first reach the threshold M_{th}; one may similarly determine the mean first time to relapse T_{rel} using Eq. (2)

$$T_{\text{rel}} = \int_0^\infty \langle S(T) \rangle dT \approx \frac{e^{\frac{2Y - \lambda}{2\kappa}}}{R_0}. \tag{35}$$

The last relationship arises from Eq. (30) and is valid for $\kappa T \gg 1$. We show T_{rel} as a function of κ in the bottom row of Fig. 9, using the same parameters chosen for $T_{\text{m}}(M)$. The mean first time to relapse is an increasing function of Y and a decreasing function of λ, indicating that positive continuous inputs and exposure to relatively small noise amplitudes can act as protective factors. These trends are consistent with those observed for $T_{\text{m}}(M)$.

3.2. The presence of cues

In this section, we study how cues affect the mental state and the likelihood of relapse. According to Eqs. (1) and (9) sensory cues are mathematically represented as a stressor of fixed amplitude w_{peak} occurring at times t_ℓ^c. This description is consistent with psychiatric studies that have identified overlaps in the neural circuits that process stress and drug-related cues and that have found that both lead to cravings and heightened susceptibility to relapse [50,57]. As mentioned earlier, we assume that cues always bring back memories of the first high so that the amplitude w_{peak} is fixed. As a result, findings illustrated in Sections 3.1.1 and 3.1.4 still hold upon substituting $B_i \to w_{\text{peak}}$ for all i and $\kappa_b \to \kappa_c$. In particular, relapse is less likely if a positive experience occurs immediately after being exposed to a drug-related cue and one can still utilize the results shown in Fig. 6 to determine the magnitude and timing of the positive experience necessary to balance exposure to a cue. Values of κ_c will be chosen such that $\kappa_c > \kappa_b$, as we expect the time to process a drug-related cue to be less than the time to overcome a stressor.

Consider the case in which an individual is randomly exposed, through a Poisson process with rate λ_c, to cues that elicit the memory of the first high. The individual thus experiences, with probability $P_c(n_c, t) = (\lambda_c t)^{n_c} e^{-\lambda_c t}/n_c!$, n_c cues within a time interval t. The mean time between successive cues is $1/\lambda_c$. Given the equivalence between cues and stressors, these results may also be interpreted as the response to an identical stressor presented at random, Poisson-distributed times. The dynamics of the cue-induced motivation is thus

$$\frac{dC}{dt} = -\kappa_c C + w_{\text{peak}} \sum_{\ell=1; t \geq t_\ell^c}^{n_c} \delta(t - t_\ell^c), \tag{36}$$

where n_c are the Poisson-distributed number of events that have occurred until time t. We also assume that there is a counteracting source of support $Y > 0$ to the mental state so that

$$M(t) = M_a(t) = \frac{Y}{\kappa_a}\left(1 - e^{-\kappa_a t}\right). \tag{37}$$

We solve Eq. (36) with the initial condition $C(t = 0) = 0$. The resulting expression for $C(t)$ can be used to write the relapse rate $R(t)$ in Eq. (1)
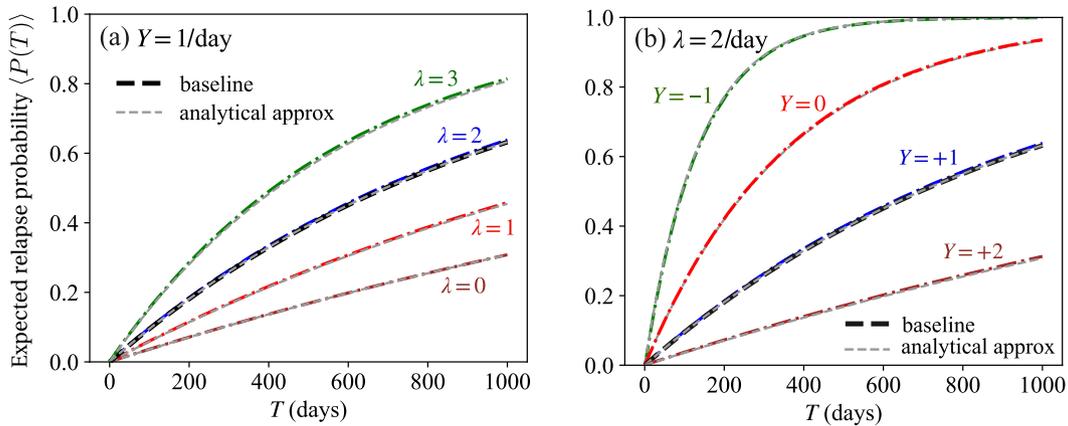
Fig. 8. Expected relapse probability $\langle P(T) \rangle$ as derived from averaging over 5000 realizations of the Ornstein–Uhlenbeck process in Eq. (19) and the analytical approximation in Eq. (30) for the baseline $Y = \lambda = 0$ with $R_0 = 10^{-3}$, $\kappa = 1$/day. Values of λ, Y displayed along the curves are in units of /day. In panel (a) we set $Y = 1$/day; as λ is increased $\langle P(T) \rangle$ also increases. For $\lambda = 2Y$ results from the baseline are recovered. Small values of $\lambda < 2Y$ decease $\langle P(T) \rangle$ below the baseline, whereas large fluctuations $\lambda > 2Y$ increase $\langle P(T) \rangle$ beyond the baseline. In panel (b) we set $\lambda = 2$/day and allow Y to be negative, representing constant negative experiences that increase $\langle P(T) \rangle$. These results indicate that sustained, large enough positive experiences may neutralize a series of random, potentially large stressors.
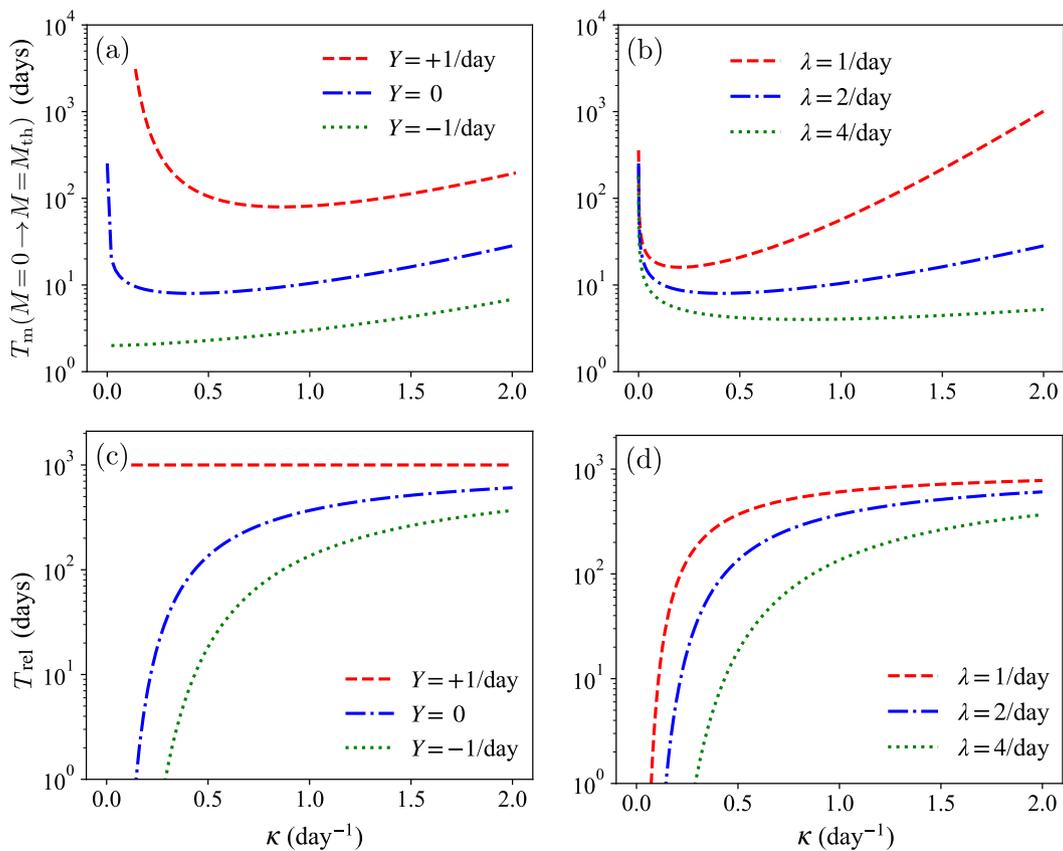
Fig. 9. Top row: Mean first passage time $T_{\mathrm{m}}(M = 0 \to M = M_{\mathrm{th}})$ for an initial mental state $M = 0$ to reach the negative threshold $M_{\mathrm{th}} = -2$ as a function of the decay rate κ. Results follow from the random process in Eq. (19) and the analytical form in Eq. (32). For large κ, each random fluctuation dissipates quickly so that the effects of multiple inputs to the mental state do not accumulate appreciably, hence $T_{\mathrm{m}}(M)$ increases with κ. Increasing κ for small values of κ will reduce the likelihood of positive values of the mental state thus shortening the time to reach M_{th} as discussed in the text. These two trends lead to the observed non-monotonic behavior, which is most pronounced for large Y, λ. In (a) we set $\lambda = 2$/day and vary the constant input Y; in (b) we set $Y = 0$ and vary the noise amplitude λ. Bottom row: Mean first passage time T_{rel} to relapse computed from the approximation in Eq. (35) and shown as a function of the decay rate κ. In panel (c) we set $\lambda = 2$/day and vary the constant input Y; in panel (d) we set $Y = 0$ and vary the noise amplitude λ.
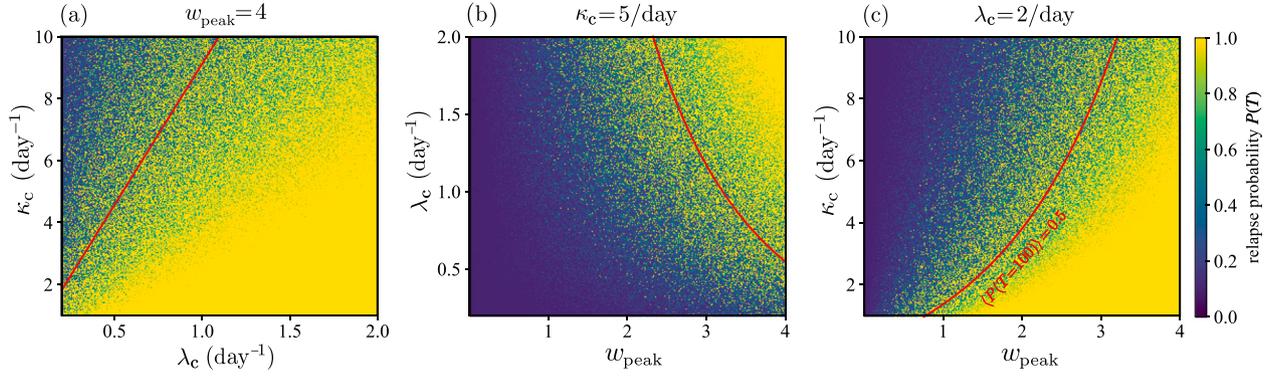
Fig. 10. Relapse probability $P(T = 100)$ following exposure to a single, randomly drawn sequence of sensory cues occurring at times generated according to a Poisson process of rate λ_c. The corresponding relapse rate is evaluated through Eq. (38) and the relapse probability at $T = 100$ days, $P(T = 100)$, is evaluated using Eqs. (2). The red curves depict the analytical approximation obtained for $\langle P(T = 100)\rangle = 0.5$ calculated using Eqs. (40) and (41). We do not include any positive, continuous form of support so that $Y = 0$ and results are independent of the processing rate κ_a. In panel (a) we fix $w_{\text{peak}} = 4$; in panel (b) we fix $\kappa_c = 5$/day; in panel (c) we fix $\lambda_c = 2$/day. Collectively, the panels show that the likelihood of relapse increases with increases in the amplitude w_{peak}, the frequency of cue occurrences λ_c, or the typical cue processing time $1/\kappa_c$.

using the mental state $M(t) = M_a(t)$ given in Eq. (37) and under the assumption that drugs are fully available $I(t) = 1$. We find

$$\frac{R(t)}{R_0} = e^{-\frac{Y}{\kappa_a}(1-e^{-\kappa_a t})} \prod_{\ell=1; t \geq t_\ell^c}^{n_c} e^{w_{\text{peak}} e^{-\kappa_c\left(t-t_\ell^c\right)}}. \tag{38}$$

Using well known properties of the Poisson process shown in the Appendix we estimate the expected value of the relapse rate for any number of events occurring within time t as

$$\left\langle \frac{R(t)}{R_0} \right\rangle = \exp\left(-\lambda_c t - \frac{Y}{\kappa_a}(1 - e^{-\kappa_a t})\right) \\ \times \exp\left[\lambda_c \int_0^t e^{w_{\text{peak}} e^{-\kappa_c(t-t')}} dt'\right]. \tag{39}$$

In the $\kappa_a t, \kappa_c t \gg 1$ limit Eq. (39) can be approximated by

$$\ln\left\langle \frac{R(t)}{R_0} \right\rangle \approx -\frac{Y}{\kappa_a} + \frac{\lambda_c}{\kappa_c}\left(\text{Ei}(w_{\text{peak}}) - \ln(w_{\text{peak}}) - \gamma\right), \tag{40}$$

where γ is the Euler–Mascheroni constant. We use the approximation in Eq. (40) to evaluate the relapse rate $R(t)$ in Eq. (2), leading to an approximate expression for $\langle P(T)\rangle$, valid for $\kappa_a T, \kappa_c T \gg 1$

$$\langle P(T)\rangle = 1 - \langle e^{-\int_0^T R(t)dt}\rangle \approx 1 - e^{-R_0 T e^{Q_c}}, \tag{41}$$

where

$$Q_c \equiv -\frac{Y}{\kappa_a} + \frac{\lambda_c}{\kappa_c}\left(\text{Ei}(w_{\text{peak}}) - \ln(w_{\text{peak}}) - \gamma\right). \tag{42}$$

In Fig. 10, we evaluate the probability of relapse at given values $\kappa_c, \lambda_c, w_{\text{peak}}$. We do this by first drawing a sequence of cues that occur according to a Poisson process of rate λ_c. Then, using this specific sequence of cues, we compute the relapse rate given in Eq. (38). Finally, we determine the survival probability and the relapse probability at a fixed time $T = 100$ days using Eq. (2). The results in Fig. 10 are obtained under the assumption of no positive input, $Y = 0$. For comparison we use the analytical approximation given in Eqs. (40) and (41) to find the parameter curve corresponding to $\langle P(T = 100)\rangle = 0.5$.

In the baseline case, where there are no cues or external stimuli, $R(t) = R_0$, hence the positive support Y will balance or alleviate the cue-induced drive to take drugs only if it satisfies

$$Y \geq \frac{\lambda_c \kappa_a}{\kappa_c}\left(\text{Ei}(w_{\text{peak}}) - \ln(w_{\text{peak}}) - \gamma\right). \tag{43}$$

Thus, to be effective, the counterbalancing source of support Y must increase with the intensity of the memory of the first high w_{peak}, the rate of exposure to the cues λ_c, the duration of the cue $1/\kappa_c$ and the processing rate of the positive events κ_a.

4. Conclusions

We presented a mathematical model for the probability of relapse in drug addiction. Our model incorporates dynamics that reflect psychiatric concepts such as the positive activation, negative activation (PA/NA) model and the peak-end rule.

Addiction research, like other studies that focus on learning, memory, rewards and synaptic plasticity, relies on neuroimaging methods to understand how the brain and its neurocircuitry adapt to short- or long-term drug use and ensuing behavioral changes. It is well documented that drug users and former users display dysregulation in their brain reward system, heightened reactivity to drug-related cues and stressors, less inhibitory self-control, and a tendency to engage in compulsive behaviors. It is also well established that the process of physical detoxification is a relatively short one, but cravings and relapse can occur even long after cessation of drug use. Relapse is often triggered by exposure to stressors or drug-related cues that the former user is unable to manage. Among the biggest limitations of neuroimaging studies and clinical trials are the need to control for individual predispositions and external circumstances, high costs, difficulties in recruiting volunteers with substance use disorder especially in longitudinal studies.

Given the complexities of addiction and the practical limitations in obtaining comprehensive data, simple and analytically tractable mathematical models may be helpful to understand how the brain responds to drugs and their absence. Decision-making and many psychiatric disorders, including addiction, have been described using quantitative mathematical models in recent years [58–63]. In our work, we considered the response of the brain to a series of inputs representing positive and negative events, and how their amplitude, timing and ordering affect the likelihood that a person in recovery will use again. By construction, and mirroring the PA/NA model, negative events increase the likelihood of relapse more than positive ones of the same magnitude. We find that clustering positive or negative events is generally detrimental. For a fixed, mental state activity integrated over a fixed time frame and imparted by an arbitrary number of negative (or positive) events, the best way of distributing these events is through a continuum of moderate negativity (or positivity), rather than as a large jolt of catastrophe (or happiness) occurring all at once. On the other hand, once an individual is exposed to a stressor, a positive event occurring immediately afterward can act as a protective factor. We also found that a constant source of positive input can balance the negativity arising from a series of random events that may include large stressors. Since the mathematical representation of sensory cues in our work is akin to that of stressors, the above considerations remain valid for exposure to drug-related cues.

The effect of different environments and user profiles may be studied by tuning relevant parameters. By changing $\kappa_a, \kappa_b, \kappa_c$ and w_{peak} we can represent users who respond differently to life experiences and whose memories of the "first high" vary in intensity. Similarly, the amplitudes A_i, B_j, the Gaussian noise λ and the Poisson parameter λ_c can represent different risk levels in the social environment of the recovering addict. Finally, although developed in the context of relapse, our model can be used to also study the driving and protective factors that lead a non-user to try drugs for the first time. In this case, $C(t) = 0$ as there are no sensory cues related to past use, but $M(t)$ can represent external stimuli that induce an individual to use drugs for the first time.

How do we translate these findings into practice? How to experience continuous positivity? Certainly, it is important to seek out positive, fulfilling experiences, embodied by the A_i events discussed in this work. However, the continuous sources of positivity we introduced, such as the green curves in Fig. 3 and the Y term in Eq. (19), represent inputs to the mental state. One may interpret these inputs as arising not just from actual events, but also as imparted from a positive attitude towards life, for example through support from family and friends, finding satisfaction in one's work, hobbies and social life. A positive attitude can also be developed through cognitive behavioral therapy, individual or group counseling or psychotherapy which are known to be effective in helping manage life's challenges without recourse to drugs.

CRediT authorship contribution statement

Sayun Mao: Formal analysis, Investigation, Methodology, Validation, Visualization, Writing – original draft, Writing – review & editing. **Tom Chou:** Conceptualization, Formal analysis, Investigation, Project administration, Supervision, Visualization, Writing – original draft, Writing – review & editing. **Maria R. D'Orsogna:** Conceptualization, Formal analysis, Funding acquisition, Investigation, Methodology, Project administration, Supervision, Visualization, Writing – original draft, Writing – review & editing.

Declaration of competing interest

The authors declare that they have no known competing financial interests or personal relationships that could have appeared to influence the work reported in this paper.

Data availability

No data was used for the research described in the article.

Acknowledgment

Appendix A. Time-dependent processing rates $\kappa_a(t)$ and $\kappa_b(t)$

Time-dependent processing rates $\kappa_a(t)$, $\kappa_b(t)$ are included in our mathematical representations of the PA/NA model in Eqs. (3a) and (3b) to allow for neuroadaptive changes after cessation of drug use. Assuming that at the beginning of the recovery phase at $t = 0$ there are no negative or positive affects so that $M_a(t = 0) = M_b(t = 0) = 0$, the general solution is

$$M_a(t) = \sum_{i, t \geq t_i^a} A_i e^{-\int_{t_i^a}^t \kappa_a(s') ds'}, \tag{A.1a}$$

$$M_b(t) = -\sum_{j, t \geq t_j^b} B_j e^{-\int_{t_j^b}^t \kappa_b(s') ds'}. \tag{A.1b}$$

Drug addiction is known to attenuate the pleasure stemming from positive stimuli, leading to anhedonia [27]. It is thus reasonable to

assume that after cessation of drug use, positive experiences will return to being more pleasurable. This is supported by experimental evidence that dopamine transporter loss in former methamphetamine users can recover after a sufficiently long period of abstinence [49]. Plausible forms for $\kappa_a(t)$ include monotonically decreasing functions that start at $\kappa_a(t = 0) = \kappa_{a,0}$ and that descend towards the standard value at full recovery $\kappa_a(t \to \infty) = \kappa_a^* < \kappa_{a,0}$. Within this scenario, positive events occurring well into the recovery phase elevate one's mental state for a longer period compared to positive events occurring at the onset of the recovery phase. Similarly, since drug abuse is known to exacerbate negative emotional distress [25,47,48,64], we can assume that $\kappa_b(t)$ is a monotonically increasing function with $\kappa_b(t = 0) = \kappa_{b,0}$ that increases towards $\kappa_b(t \to \infty) = \kappa_b^* > \kappa_{b,0}$. In this case, negative affects linger less in the minds of former users as recovery continues. We mathematically represent the processing rates $\kappa_a(t), \kappa_b(t)$ during abstinence as

$$\kappa_a(t) = \kappa_{a,0} e^{-\gamma_a t} + \kappa_{a*}(1 - e^{-\gamma_a t}), \tag{A.2a}$$

$$\kappa_b(t) = \kappa_{b,0} e^{-\gamma_b t} + \kappa_{b*}(1 - e^{-\gamma_b t}), \tag{A.2b}$$

where $\gamma_a^{-1}, \gamma_b^{-1}$ are typical time scales associated with neuroadaptive changes to the processing rates and where $\kappa_{a,0} > \kappa_a^*$ and $\kappa_{b,0} < \kappa_b^*$. The positive affect $M_a(t)$ in Eq. (A.1a) can thus be written as

$$M_a(t) = \sum_{i, t \geq t_i^a} A_i e^{-\kappa_a^*(t-t_i^a)} \exp\left[\frac{(\kappa_a^* - \kappa_{a,0})}{\gamma_a}\left(e^{-\gamma_a t_i^a} - e^{-\gamma_a t}\right)\right]. \tag{A.3}$$

For $M_b(t)$ in Eq. (A.1b) instead we find

$$M_b(t) = -\sum_{j, t \geq t_j^b} B_j e^{-\kappa_b^*(t-t_j^b)} \exp\left[\frac{(\kappa_b^* - \kappa_{b,0})}{\gamma_b}\left(e^{-\gamma_b t_j^b} - e^{-\gamma_b t}\right)\right]. \tag{A.4}$$

If the restoring, neuroadaptive changes to $\kappa_a(t)$ occur over short time scales such that $\gamma_a t_i^a \gg 1$, then $\kappa_a(t)$ can be approximated by its equilibration value κ_a^*. Conversely, for longer lived changes scales such that $\gamma_a t_i^a \ll 1$, then $\kappa_a(t)$ can be approximated by its initial condition $\kappa_{a,0}$. In either of these two limits, $\kappa_a(t)$ can be approximated by a constant, κ_a. Similar considerations hold for $\kappa_b(t)$ that in the same limits can be modeled as a constant κ_b. We can thus write

$$M_a(t) = \sum_{i, t \geq t_i^a} A_i e^{-\kappa_a(t-t_i^a)}, \quad M_b(t) = -\sum_{j, t \geq t_j^b} B_j e^{-\kappa_a(t-t_j^b)}, \tag{A.5}$$

where $\kappa_a = \kappa_{a,0}$ or κ_a^* depending on the proper limit (and similarly for κ_b) and use the results for the constant κ_a, κ_b cases discussed in Eq. (4).

Instead of considering a sequence of positive or negative events, for simplicity, we now assume there is a constant negative input $Y = -0.5/\text{day}$ and that there are no random events. In this scenario, the ideal case of an individual who has never used drugs is represented by the negative mental state $M(t) = M_b(t)$ given by

$$M(t) = \frac{Y}{\kappa_b^*}(1 - e^{-\kappa_b^* t}), \tag{A.6}$$

and obtained using the standard processing rate κ_b^*. We identify the scenario of a recovering addict processing events with the same rates as if drugs were never used, as a proxy for full recovery. A patient still in recovery on the other hand processes events at the time-dependent rate $\kappa_b(t)$ given by Eq. (A.2b). For this individual, the same circumstances yield the following negative mental state

$$M(t) = Y e^{-\int_0^t \kappa_b(t') dt'} \int_0^t e^{\int_0^{t'} \kappa_b(t'') dt''} dt'. \tag{A.7}$$

Eq. (A.7) reduces to Eq. (A.6) under no recovery, when $\gamma_b = 0$ in Eq. (A.7), provided κ_b^* is replaced by $\kappa_{b,0}$ in Eq. (A.6).

In Fig. A.11 we consider a dynamically varying $\kappa_b(t)$ and plot the mental state $M(t)$ and relapse probability $P(t)$ for an initial processing rate $\kappa_{0,b} = 1/\text{day}$ and the recovered, standard processing rate $\kappa_b^* = 2/\text{day}$. The initially large value of $\kappa_{0,b}$ implies that right after cessation of drug use the neurocircuitry of the individual is still compromised, and any life event is processed quickly. We also set $\gamma_b = 0.002/\text{day}$,
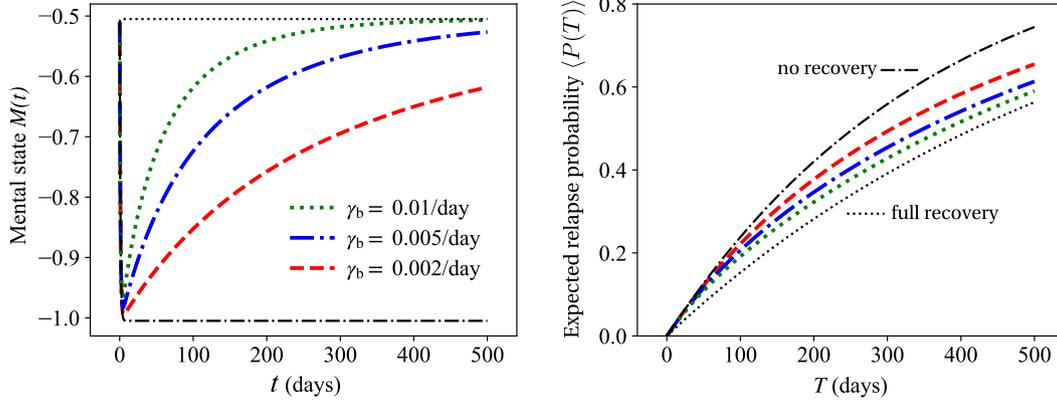
Fig. A.11. Dynamics of $M(t)$ and $\langle P(T) \rangle$ under a continuous negative input $Y = -0.5$/day, an initial processing rate $\kappa_{b,0} = 1$/day, a fully recovered processing rate $\kappa_b^* = 2$/day, and $R_0 = 10^{-3}$. Recovery rates are given by $\gamma_b = 0.002, 0.005, 0.01$/day. The black dashed curve is the ideal case of the individual never having used drugs, or having fully recovered (Eq. (A.6)), and the dotted curve is the no recovery case ($\gamma_b = 0$ in Eq. (A.7)). Intermediate curves show patients in recovery who tend to approach the ideal case of never having used drugs after a long enough recovery time.

$\gamma_b = 0.005$/day and $\gamma_b = 0.01$/day, corresponding to recovery times from $\kappa_{0,b}$ to κ_b^* ranging from three months to one and half years, approximately.

The mental states $M(t)$ in each of these scenarios are shown in Fig. A.11(a). In Fig. A.11(b) we show the corresponding expected relapse probability, $\langle P(T) \rangle$. Here, the state of no exposure to drugs (Eq. (A.6)) is represented by the lower-bounded curve and the state of no recovery from drugs (Eq. (A.7) with $\gamma_b = 0$) is represented by the upper-bounded one. All other curves correspond to Eq. (A.7) with finite, non-zero values of the recovery rate γ_b. As can be seen, the latter are all initially closer to the upper bound, as the recovery effects are minimal at the onset. However, as the recovery process continues, the curves start approaching the lower curve corresponding to the ideal case of the individual never having used drugs in the first place. Finally, faster recovery processes (larger values of γ_b) yield lower relapse probabilities.

Appendix B. Estimating the relapse probability

Here, we consider approximations to the expected relapse probability $\langle P(T) \rangle$ as given by Eq. (29)

$$\langle P(T) \rangle = 1 - \langle S(T) \rangle = 1 - \left\langle \exp\left[-R_0 \int_0^T e^{-M(t')} dt' \right] \right\rangle. \tag{B.1}$$

We first expand the exponential in Eq. (B.1) in a Taylor series

$$\langle S(T) \rangle = \sum_{n=0}^{\infty} \frac{R_0^n}{n!} (-1)^n \int_0^T \cdots \int_0^T \langle e^{-M(t^{(1)})} \cdots e^{-M(t^{(n)})} \rangle dt^{(1)} \cdots dt^{(n)} \tag{B.2}$$

and note that upon neglecting correlations we can approximate the expectation of the products of $e^{-M(t)}$ in Eq. (B.2) as products of expectations so that

$$\int_0^T \cdots \int_0^T \langle e^{-M(t^{(1)})} \cdots e^{-M(t^{(n)})} \rangle dt^{(1)} \cdots dt^{(n)} \approx \left[\int_0^T \langle e^{-M(t)} \rangle dt \right]^n, \tag{B.3}$$

leading to

$$\langle P(T) \rangle \approx 1 - \exp\left[-R_0 \int_0^T \langle e^{-M(t)} \rangle dt \right]. \tag{B.4}$$

We now evaluate the integral for the $n = 1$ summand in Eq. (B.2), for which Eq. (B.3) is exact. We find

$$\langle e^{-M(t)} \rangle = \int_{-\infty}^{\infty} e^{-M} P_m(M, t) \, dM$$

$$= \exp\left(\frac{\lambda - 2Y}{2\kappa} \right) \exp\left[-\left(M_0 - \frac{Y}{\kappa} \right) e^{-\kappa t} - \frac{\lambda}{2\kappa} e^{-2\kappa t} \right]. \tag{B.5}$$

We now consider the $n = 2$ summand in Eq. (B.2) to determine the conditions under which the approximation in Eq. (B.3) fails and

correlations must be taken into account. Our goal is thus to evaluate $\langle e^{-M(t^{(1)})} e^{-M(t^{(2)})} \rangle \equiv \langle e^{-M(t')} e^{-M(t'')} \rangle$. To do this, we must consider the joint probability density $P_m(M_1, M_2, t', t'')$ of finding the mental state M_1 at time t' and of finding the mental state M_2 at time $t'' > t'$, conditioned on the previous value M_1 at time t'. This is given by

$$P_m(M_1, M_2, t', t'') = P_m(M_2, t''|M_1, t') P_m(M_1, t'), \tag{B.6}$$

where $P_m(M_1, t')$ is the probability density of finding M_1 at t', with the given initial conditions, and where $P_m(M_2, t'|M_1, t')$ is the probability density of finding M_2 at t'', conditioned on having M_1 at t'. The two quantities evolve according to the Fokker–Planck equation shown in Eq. (23) and lead to

$$\langle e^{-M(t')} e^{-M(t'')} \rangle$$

$$= \int_{-\infty}^{\infty} \int_{-\infty}^{\infty} e^{-M_1} e^{-M_2} P_m(M_2, M_1, t', t'') dM_1 dM_2$$

$$= \int_{-\infty}^{\infty} \int_{-\infty}^{\infty} e^{-M_1} e^{-M_2} P_m(M_2, t''|M_1, t') P_m(M_1, t') dM_1 dM_2, \tag{B.7}$$

where

$$P_m(M_1, t') \sim \mathcal{N}\left(\mu_1(t'), \ \sigma^2(t') \right),$$

$$P_m(M_2, t''|M_1, t') \sim \mathcal{N}\left(\mu_2(t'' - t'), \ \sigma^2(t'' - t') \right), \tag{B.8}$$

and $\mathcal{N}(\mu, \sigma)$ is the normal distribution of mean μ and variance σ. The values μ_1, μ_2, σ are given by

$$\mu_1(t') = \frac{Y}{\kappa} + \left(M_0 - \frac{Y}{\kappa} \right) e^{-\kappa t'},$$

$$\mu_2(t'' - t') = \frac{Y}{\kappa} + \left(M_1 - \frac{Y}{\kappa} \right) e^{-\kappa(t'' - t')},$$

$$\sigma^2(t) = \frac{\lambda}{\kappa}(1 - e^{-2\kappa t}). \tag{B.9}$$

We now evaluate Eq. (B.7) to find

$$\langle e^{-M(t')} e^{-M(t'')} \rangle = \langle e^{-M(t')} \rangle \langle e^{-M(t'')} \rangle e^{\frac{2\lambda}{\kappa} e^{-\kappa t''} \sinh(\kappa t')}, \tag{B.10}$$

where $\langle e^{-M(t')} \rangle$ is given in Eq. (B.5). Given that $t'' > t'$, the exponential term in Eq. (B.10) will tend towards unity as $\kappa \to \infty$, implying correlations can be neglected. The $\kappa \to \infty$ limit corresponds to a relatively short processing time, consistent with the notion that the decay of random events is fast and do not allow for strong correlations. Conversely, if $\kappa \to 0$ we find

$$\lim_{\kappa \to 0} \exp\left(\frac{2\lambda}{\kappa} e^{-\kappa t''} \sinh(\kappa t') \right) = e^{2\lambda t'}, \tag{B.11}$$

which can be quite large for even moderate values of λ at large times. Finally, note that if we set $2\lambda = \alpha\kappa$ where α is a proportionality constant, then

$$\lim_{\kappa \to 0} \exp\left(\alpha e^{-\kappa t''} \sinh(\kappa t') \right) = 1, \tag{B.12}$$
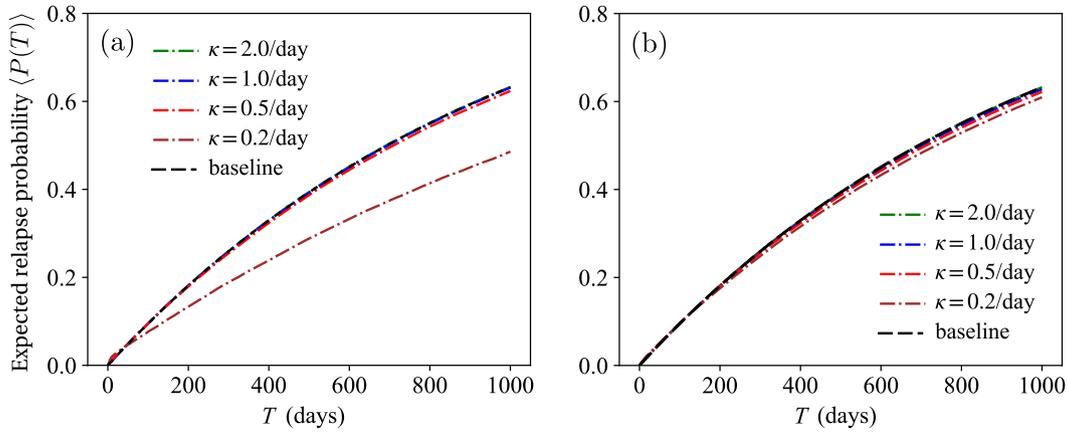
Fig. B.12. Expected relapse probability $\langle P(T) \rangle$ as determined from 5000 trajectories of the Ornstein–Uhlenbeck process with $M_0 = 0$ and various parameters Y, λ, κ and the analytical estimate given by Eqs. (30) and (26a). The ratio $\lambda = 2Y$ is kept for all parameter combinations, leading to the expectation $\langle P(T) \rangle \approx 1 - \exp(R_0 T)$, according to Eq. (30). In panel (a) we fix $Y = 1$/day and $\lambda = 2$/day. Results from the numerical simulations match the analytical estimate only for large values of κ as illustrated in the text, when correlations can be neglected. In panel (b) we fix $2\lambda = \alpha\kappa$, with $\alpha = 8$ to show that under this assumption correlations play a less prominent role in the limit $\kappa \to 0$.

suggesting that an alternative way of neglecting correlations in the small κ limit, when the processing time is large, is to instead modulate the amplitude of the noise λ to be comparable to κ. The evaluation of higher order correlations $n > 2$ in Eq. (B.2) is a more tedious calculation, but we expect that in the $\kappa \to \infty$ limit the same considerations will apply and that correlations can also be neglected. In Fig. B.12 we plot the expected relapse probability $\langle P(T) \rangle$ obtained by averaging over 5,000 runs of the Ornstein–Uhlenbeck process for several values of κ and other parameters. We show that the analytical approximation in Eq. (30) holds only for sufficiently large values of κ.

Appendix C. Deriving the average relapse rate for Poisson distributed cues

We now derive Eq. (39) assuming cues affect the mental state M through events of amplitude w_{peak} that are Poisson distributed with rate λ_c. According to Eq. (38), assuming that within time t there have been n_c Poisson distributed cues, the relapse rate is given by

$$\frac{R(t)}{R_0} = \exp\left[-\frac{Y}{\kappa_a}\left(1 - e^{-\kappa_a t}\right)\right] \prod_{\ell=1; t \geq t_\ell^c}^{n_c} \exp\left[w_{\text{peak}} e^{-\kappa_c\left(t - t_\ell^c\right)}\right]. \quad \text{(C.1)}$$

For a general function $f(y)$ one can show that given n_c events within time t that are Poisson distributed, the following holds

$$\left\langle \prod_{\ell=1}^{n_c} f(t_\ell^c) \right\rangle \bigg|_{n_c} = \left[\frac{1}{t} \int_0^t f(y)\mathrm{d}y\right]^{n_c}, \quad n_c \sim \text{Poisson}(\lambda_c, t). \quad \text{(C.2)}$$

We will show the validity of this expression below. For now, assuming Eq. (C.2) holds, we write

$$\left\langle \frac{R(t)}{R_0} \right\rangle \bigg|_{n_c} = \exp\left[-\frac{Y}{\kappa_a}\left(1 - e^{-\kappa_a t}\right)\right] \left[\frac{1}{t} \int_0^t \exp\left[w_{\text{peak}} e^{-\kappa_c(t-t')}\right] \mathrm{d}t'\right]^{n_c}. \quad \text{(C.3)}$$

We can now average over the likelihood of having n_c events within t by weighting Eq. (C.3) by the Poisson distribution to obtain

$$\left\langle \frac{R(t)}{R_0} \right\rangle = \exp\left[-\frac{Y}{\kappa_a}\left(1 - e^{-\kappa_a t}\right)\right]$$
$$\times \sum_{n_c=0}^\infty \frac{(\lambda_c t)^{n_c} e^{-\lambda_c t}}{n_c!} \left[\frac{1}{t} \int_0^t \exp\left[w_{\text{peak}} e^{-\kappa_c(t-t')}\right] \mathrm{d}t'\right]^{n_c}. \quad \text{(C.4)}$$

Upon evaluating the integral above we write

$$\left\langle \frac{R(t)}{R_0} \right\rangle = \exp\left[-\lambda_c t - \frac{Y}{\kappa_a}\left(1 - e^{-\kappa_a t}\right) + \lambda_c \int_0^t e^{w_{\text{peak}} e^{-\kappa_c(t-t')}} \mathrm{d}t'\right], \quad \text{(C.5)}$$

which, for $\kappa_a t, \kappa_c t \gg 1$ can be simplified to

$$\lim_{t \to \infty} \ln \left\langle \frac{R(t)}{R_0} \right\rangle = -\frac{Y}{\kappa_a} + \frac{\lambda_c}{\kappa_c}\left(\text{Ei}(w_{\text{peak}}) - \ln(w_{\text{peak}}) - \gamma\right), \quad \text{(C.6)}$$

where γ is the Euler–Mascheroni constant. To show the validity of Eq. (C.2) we take a general Poisson process of rate η and for which $p(t_1, \ldots, t_n | N = n)$ is the probability density of n events occurring within time t ordered such that $t_1 \leq t_2 \leq \cdots \leq t_n$. In a Poisson process, the possibility of an event occurring in $[t, t + \mathrm{d}t]$ is always $\eta \mathrm{d}t$, which does not correlate with time, so we can divide the time period t equally into M segments of length $\mathrm{d}t$ with $M \gg 1$ so that $t = M\mathrm{d}t$. We label them $\{[T_1, T_1+\mathrm{d}t], [T_2, T_2+\mathrm{d}t], \ldots, [T_M, T_M+\mathrm{d}t]\}$. Since each event $t_1 \leq t_k \leq t_n$ will fall into one of the above segments we can write

$$p(t_1, \ldots, t_n | N = n)(\mathrm{d}t)^n$$
$$= \mathbb{P}(T_1 < t_1 < T_1 + \mathrm{d}t, \ldots, T_n < t_n < T_n + \mathrm{d}t) \quad \text{(C.7)}$$
$$= \mathbb{P}(\{[T_1, T_1 + \mathrm{d}t], \ldots, [T_n, T_n + \mathrm{d}t]\}),$$

where the last equality implies that one can simply pick the $n \in M$ segments corresponding to the $t_1 \leq t_k \leq t_n$ events. Since these intervals are equiprobable, and

$$p(t_1, \ldots, t_n | N = n)(\mathrm{d}t)^n = \binom{M}{n}^{-1} = \frac{n!(M-n)!}{M!} \approx \frac{n!}{M^n}.$$

Using $M = t/\mathrm{d}t$, this becomes $p(t_1, \ldots, t_n | N = n) = \frac{n!}{t^n}$. An alternative way to obtain this is result is to use the explicit form for the Poisson distribution

$$p(t_1, \ldots, t_n | N = n) = \frac{p(t_1, \ldots, t_n, N = n)}{P(N = n)}$$
$$= \frac{e^{-\eta(T-t_n)} \cdot \eta e^{-\eta(t_n - t_{n-1})} \cdots \eta e^{-\eta(t_1 - t_2)} \cdot \eta e^{-\eta t_1}}{\frac{(\eta T)^n e^{-\eta T}}{n!}} \quad \text{(C.8)}$$
$$= \frac{\eta^n e^{-\eta T}}{\frac{(\eta T)^n e^{-\eta T}}{n!}} = \frac{n!}{T^n}.$$

Finally, for a generic function $f(t)$ and for a series of n Poisson-distributed events occurring at times $0 < t_1 < \cdots < t_n < t$ we can write

$$\left\langle \prod_{j=1}^n f(t_j) \right\rangle \bigg|_n = \int \left[\prod_{j=1}^n f(t_j) p(t_1, \ldots, t_n | N = n)\right] \mathrm{d}t_1 \cdots \mathrm{d}t_n$$
$$= \frac{n!}{t^n} \int \left[\prod_{j=1}^n f(t_j)\right] \mathrm{d}t_1 \cdots \mathrm{d}t_n = \frac{n!}{t^n} \int \left[\prod_{j=1}^n f(t_j)\mathrm{d}t_j\right],$$

where the multidimensional time integrals are constrained by $0 < t_1 < \cdots < t_n < t$. We now eliminate the ordering of the sequence $t_1, \ldots, t_n$,

and divide the integral by the number of permutations to obtain

$$\left\langle \prod_{j=1}^{n} f(t_j) \right\rangle \Bigg|_n = \frac{1}{t^n} \left[\prod_{j=1}^{n} \int_{0 < t_j < t} f(t_j) \mathrm{d}t_j \right]$$

$$= \prod_{j=1}^{n} \left[\int_0^t f(t_j) \frac{\mathrm{d}t_j}{t} \right] = \frac{1}{t} \left[\int_0^t f(y) \mathrm{d}y \right]^n,$$

which is Eq. (C.2).

References

[1] Farida Bhuiya Ahmad, Jodi A. Cisewski, Lauren M. Rossen, Paul Sutton, Provisional Drug Overdose Death Counts, National Center for Health Statistics, 2022.

[2] U.S. Department of Health and Human Services, Substance Abuse and Mental Health Services Administration, Center for Behavioral Health Statistics and Quality, NSDUH-2021-DS0001, National Survey on Drug Use and Health 2021, 2021, https://datafiles.samhsa.gov.

[3] Nora D. Volkow, Marisela Morales, The brain on drugs: From reward to addiction, Cell 162 (4) (2015) 712–725.

[4] National Institute on Drug Abuse, Treatment and recovery, 2022, https://nida.nih.gov/publications/drugs-brains-behavior-science-addiction/treatment-recovery.

[5] A. Thomas McLellan, David C. Lewis, Charles P. O' Brien, Herbert D. Kleber, Drug dependence, a chronic medical illness: Implications for treatment, insurance, and outcomes evaluation, JAMA 284 (2000) 1689–1695.

[6] Rajita Sinha, New findings on biological factors predicting addiction relapse vulnerability, Curr. Psychiatry Rep. 13 (2011) 398–405.

[7] Mary L. Brecht, Diane Herbeck, Time to relapse following treatment for methamphetamine use: A long-term perspective on patterns and predictors, Drug Alcohol Depend. 139 (2014) 18–25.

[8] Bobby P. Smyth, Joseph Barry, Eamon Keenan, Kevin Ducray, Lapse and relapse following inpatient treatment of opiate dependence, Irish Med. J. 103 (2010) 176–179.

[9] Alan David Kaye, Richard D. Urman, Elyse M. Cornett Cornett, Amber Edinoff, Substance Use and Addiction Research: Methodology, Mechanisms, and Therapeutics, Academic Press, London, UK, 2023.

[10] Maria R. D'Orsogna, Lucas Böttcher, Tom Chou, Fentanyl-driven acceleration of racial, gender and geographical disparities in drug overdose deaths in the United States, PLOS Glob. Public Health 3 (2023) e0000769.

[11] Daniele Caprioli, Michele Celentano, Giovanna Paolone, Aldo Baldiani, Modeling the role of environment in addiction, Progress Neuro-Psychopharmacol. Biol. Psychiatry 31 (2007) 1639–1653.

[12] Nora D. Volkow, Joanna S. Fowler, Gene-Jack Wang, The addicted human brain: Insights from imaging studies, J. Clin. Investig. 111 (2003) 1444–1451.

[13] George F. Koob, Nora D. Volkow, Neurocircuitry of addiction, Neuropsychopharmacol.: Official Publ. Am. College Neuropsychopharmacol. 35 (1) (2010) 217–238.

[14] Rita Z. Goldstein, Nora D. Volkow, Dysfunction of the prefrontal cortex in addiction: neuroimaging findings and clinical implications, Nat. Rev. Neurosci. 12 (11) (2011) 652–669.

[15] George F. Koob, Nora D. Volkow, Neurobiology of addiction: A neurocircuitry analysis, Lancet. Psychiatry 3 (2016) 760–773.

[16] Jessica A. Mollick, Hedy Kober, Computational models of drug use and addiction: A review, J. Abnormal Psychol. 129 (2020) 544–555.

[17] Tom Chou, Maria R. D'Orsogna, A mathematical model of reward-mediated learning in drug addiction, Chaos 32 (2022) 021102.

[18] Boris S. Gutkin, Stanislas Dehaene, Jean P. Changeux, A neurocomputational hypothesis for nicotine addiction, Proc. Natl. Acad. Sci. 103 (2006) 1106–1111.

[19] Abraham Peper, Intermittent adaptation: A mathematical model of drug tolerance, dependence and addiction, in: Boris S. Gutkin, Serge H. Ahmed (Eds.), Computational Neuroscience of Drug Addiction, in: Springer Series in Computational Neuroscience, vol. 10, Springer, New York, NY, 2012, pp. 19–56, chapter 2.

[20] Hawre Jalal, Jeanine M. Buchanich, Mark S. Roberts, Lauren C. Balmert Balmert, Kun Zhang Zhang, Donald S. Burke, Changing dynamics of the drug overdose epidemic in the United States from 1979 through 2016, Science 361 (2018) 6408.

[21] Lucas Böttcher, Tom Chou, Maria R. D'Orsogna, Modeling and forecasting age-specific overdose mortality in the United States, Eur. Phys. J. Spec. Top. 232 (2023) 1743–1752.

[22] Lucas Böttcher, Tom Chou, Maria R. D'Orsogna, Forecasting drug-overdose mortality by age in the United States at the national and county levels, PNAS Nexus 3 (2024) pgae050.

[23] Rajita Sinha, How does stress increase risk of drug abuse and relapse? Psychopharmacology 158 (2001) 343–359.

[24] Christopher J. Evans, Catherine M. Cahill, Neurobiology of opioid dependence in creating addiction vulnerability, F1000Research 5 (2016) 1748.

[25] George F. Koob, Neurobiology of opioid addiction: Opponent process, hyperkatifeia, and negative reinforcement, Biol. Psychiat. 87 (2020) 44–53.

[26] Lili Nie, Dara G. Ghahremani, Mark A. Mandelkern, Andy C. Dean, Wei Luo, Anlian Ren, Jing Li, Edythe D. London, The relationship between duration of abstinence and gray-matter brain structure in chronic methamphetamine users, Am. J. Drug Alcohol Abuse 47 (2021) 65–73.

[27] George F. Koob, Anhedonia, hyperkatifeia, and negative reinforcement in substance use disorders, in: Diego A. Pizzagalli (Ed.), Anhedonia: Preclinical, Translational, and Clinical Integration, Springer, Cham, Switzerland, 2022.

[28] Nilofar Vafaie, Hedy Kober, Association of drug cues and craving with drug use and relapse; A systematic review and meta-analysis, JAMA Psychiatry 79 (2022) 641–650.

[29] Daniel L. Kahneman, Evaluation by moments, past and future, in: Choices, Values and Frames, Cambridge University Press, 2000, pp. 693–708.

[30] Barbara L. Fredrickson, Daniel L. Kahneman, Duration neglect in retrospective evaluations of affective episodes, J. Personal. Soc. Psychol. 65 (1993) 45–55.

[31] Aaron M. Bornstein, Hanna Pickard, "Chasing the first high": Memory sampling in drug choice, Neuropsychopharmacology 45 (2020) 907–915.

[32] Sean E. McCabe, James A. Cranford, Carol J. Boyd, Stressful events and other predictors of remission from drug dependence in the United States: Longitudinal results from a national survey, J. Subst. Abuse Treat. 71 (2016) 41–47.

[33] Christina J. Perry, Isabel Zbukvic, Jee H. Kim, Andrew J. Lawrence, Role of cues and contexts on drug-seeking behaviour, Br. J. Pharmacol. 171 (2014) 4636–4672.

[34] Rajtarun Madangopal, Brendan J. Tunstall, Lauren E. Komer, Sophia J. Weber, Jennifer K. Hoots, Veronica A. Lennon, Jennifer M. Bossert, David H. Epstein, Yavin Shaham, Bruce T. Hope, Discriminative stimuli are sufficient for incubation of cocaine craving, eLife 8 (2019) e44427.

[35] Freidbert Weiss, Roberto Ciccocioppo, Loren H. Parsons, Simon Katner, Xiu Liu, Eric P. Zorrilla, Glenn R. Valdez, Osnat Ben-Shahar, Stefania Angeletti, Regina R. Richter, Compulsive drug-seeking behavior and relapse. Neuroadaptation, stress, and conditioning factors, Ann. New York Acad. Sci. 937 (2001) 1–26.

[36] George F. Koob, Michel Le Moal, Neurobiological mechanisms for opponent motivational processes in addiction, Philos. Trans. R. Soc. B 363 (1507) (2008) 3113–3123.

[37] Mehdi Keramati, Boris S. Gutkin, Homeostatic reinforcement learning for integrating reward collection and physiological stability, eLife 3 (2014) e04811.

[38] Theodora Duka, Hans S. Crombag, David N. Stephens, Experimental medicine in drug addiction: Towards behavioral, cognitive and neurobiological biomarkers, J. Psychopharmacol. 25 (2011) 1235–1255.

[39] David Watson, David Wiese, Jatin Vaidya, Auke Tellegen, The two general activation systems of affect: Structural findings, evolutionary considerations, and psychobiological evidence, J. Personal. Soc. Psychol. 76 (1999) 820–838.

[40] James J. Gross, Robert W. Levenson, Emotion elicitation using films, Cognit. Emotion 9 (1995) 87–108.

[41] Tiffany A. Ito, John T. Cacioppo, Peter J. Lang, Eliciting affect using the international affective picture system: Trajectories through evaluative space, Pers. Soc. Psychol. Bull. 24 (1998) 855–879.

[42] John T. Cacioppo, W.L. Gardner, G.G. Berntson, The affect system has parallel and integrative processing components: Form follows function, J. Personal. Soc. Psychol. 76 (1999) 839–855.

[43] Peter J. Lang, The emotion probe. Studies of motivation and attention, Am. Psychol. 50 (1995) 372–385.

[44] Tiffany A. Ito, Jeff T. Larsen, N. Kyle Smith, John T. Cacioppo, Negative information weighs more heavily on the brain: The negativity bias in evaluative categorizations, J. Personal. Soc. Psychol. 75 (1998) 887–900.

[45] Noam Zilberman, Gal Yadid, Yaniv Efrati, Yuri Rassovsky, Negative and positive life events and their relation to substance and behavioral addictions, Drug Alcohol Depend. 204 (2019) 107562.

[46] Noam Zilberman, Gal Yadid, Yaniv Efrati, Yuri Rassovsky, Who becomes addicted and to what? Psychosocial predictors of substance and behavioral addictive disorders, Psychiatry Res. 291 (2020) 113221.

[47] George F. Koob, Patricia Powell, Aaron White, Addiction as a coping response: Hyperkatifeia, deaths of despair, and COVID-19, Am. J. Psychiatry 177 (2020) 1031–1037.

[48] George F. Koob, Drug addiction: Hyperkatifeia/Negative reinforcement as a framework for medications development, Pharmacol. Rev. 73 (2021) 163–201.

[49] Nora D. Volkow, Linda Chang, Gene-Jack Wang, Joanna S. Fowler, Dinko Franceschi, Mark Sedler, Samuel J. Gatley, Eric Miller, Robert Hitzemann, Yu-Shin Ding, et al., Loss of dopamine transporters in methamphetamine abusers recovers with protracted abstinence, J. Neurosci. 21 (23) (2001) 9414–9418.

[50] Rajita Sinha, Chaing-Shan Ray Li, Imaging stress- and cue-induced drug and alcohol craving: Association with relapse and clinical implications, Drug Alcohol Rev. 26 (2007) 25–31.

[51] Helen C. Fox, Keri L. Bergquist, Kwang I. Hong, Rajita Sinha, Stress-induced and alcohol cue-induced craving in recently abstinent alcohol dependent individuals, Alcohol Clin. Exp. Res. 31 (2007) 395–403.

[52] Kyle Kampman, Margaret Jarvis, National practice guideline for the use of medications in the treatment of addiction involving opioid use, J. Addiction Med. 9 (2015) 358–367.

[53] George E. Uhlenbeck, Leonard S. Ornstein, On the theory of Brownian motion, Phys. Rev. 36 (1930) 823–841.

[54] Crispin W. Gardiner, Handbook of Stochastic Methods, fourth ed., Springer-Verlag, Berlin, 2009.

[55] Hannes Risken, The Fokker–Planck Equation: Methods of Solution and Applications, Springer-Verlag, New York, 1989.

[56] Caibin Zeng, Mean exit time and escape probability for the Ornstein–Uhlenbeck process, Chaos 30 (9) (2020) 093127.

[57] Helen C. Fox, Makram Talih, Robert Malison, George M. Anderson, Mary J. Kreek, Rajita Sinha, Frequency of recent cocaine and alcohol use affects drug craving and associated responses to stress and drug-related cues, Psychoneuroendocrinology 30 (2005) 880–891.

[58] Christophe Gauld, Damien Depannemaecker, Dynamical systems in computational psychiatry: A toy-model to apprehend the dynamics of psychiatric symptoms, Front. Psychol. 14 (2023) 1099257.

[59] Olena Trofymchuk, Eduardo Liz, Sergei Trofimchuk, The peak-end rule and its dynamic realization through differential equations with maxima, Nonlinearity 36 (2023) 507–536.

[60] Xiaoou Cheng, Maria R. D'Orsogna, Tom Chou, Mathematical modeling of depressive disorders: Circadian driving, bistability and dynamical transitions, Comput. Struct. Biotechnol. J. 19 (2020) 664–690.

[61] Tobias U. Hauser, Vasilisa Skvortsova, Munmun De Choudhury, Nikolaos Koutsouleris, The promise of a model-based psychiatry: Building computational models of mental ill health, Lancet Digit. Health 4 (2022) e816–e828.

[62] Lae U. Kim, Maria R. D'Orsogna, Tom Chou, Onset, timing, and exposure therapy of stress disorders: Mechanistic insight from a mathematical model of oscillating neuroendocrine dynamics, Biol. Direct 11 (2016) 13.

[63] Rosemary Harris, Random walkers with extreme value memory: Modeling the peak-end rule, New J. Phys. 17 (2015) 053049.

[64] Ali Cheetham, Nicholas B. Allen, Murat Yucel, Dan I. Lubman, The role of affective dysregulation in drug addiction, Clin. Psychol. Rev. 30 (2010) 621–634.